Title: Whole-genome analyses point to new candidate genes underlying aestivation in amphibians

Running head: New candidate genes underlying aestivation in amphibians

Authors: Leticia M. Ochoa-Ochoa[1,2,*+], Rebecca D. Tarvin[2,+]

1. Museo de Zoología Alfonso L. Herrera, Department of Evolutionary Biology, Faculty of Sciences, Universidad Nacional Autónoma de México (UNAM), 04510, Ciudad de México, México.
2. Museum of Vertebrate Zoology and Department of Integrative Biology, University of California, Berkeley, Berkeley, CA 94720 USA.

+ Contributed equally to this work

***Corresponding author:** leticia.ochoa@ciencias.unam.mx

What is already known

Over 300 million years ago, the ancestors of amphibians were the first vertebrates to emerge onto land, and they likely experienced intense physiological stresses. To this day, many amphibians have retained the ability to survive water and heat stress through aestivation, a hypometabolic state during which animals suspend their daily activities. How aestivation is induced and maintained is of medical interest because these animals can live in suspended animation for months or even years at a time, while retaining the ability to awaken without organ atrophy or cancerous tissues. The genetics of aestivation are just beginning to be understood, but much remains to be discovered.

What this study adds

This study uses newly available genomic resources for amphibians and new genome-wide analysis tools to provide novel insight into the genes and processes underlying aestivation. The genome-wide assessment and inclusion of species not previously studied from a genetic perspective provides novel candidate processes involved in aestivation like angiogenesis and protein and membrane trafficking. The diversity of amphibians that aestivate is much greater than in other vertebrate groups and represents a relatively untapped resource that can inspire future innovations in human medicine.

Acknowledgments

Thanks to Craig Franklin, Rebecca Cramp, and Nicholas Hudson for sharing raw results from their 2024 publication.

Funding

Funding from UC Berkeley (BEARS) covered visiting scholar expenses. Funding was provided by the Dirección General de Asuntos del Personal Académico (DGAPA, UNAM) through the Support Program for the Improvement of Academic Personnel for sabbatical stays granted to LMOO. We also thank CONAHCYT for the scholarship received within the framework of the Complementary Support program for Sabbatical Stays Linked to the Consolidation of Research Groups also granted to LMOO.

Keywords: dormancy, glycolysis, metabolism, oxidative phosphorylation, protein trafficking, TRAPP complex.

Abstract (250)

When amphibians invaded the terrestrial realm, they likely needed a strategy such as aestivation to survive water and oxygen stress in the novel environment. In fact, aestivation appears to be an ancestral state in amphibians. We conducted a literature review about the genes previously linked to aestivation and then we searched for additional candidate genes related to the aestivation phenotype by comparing evolutionary rates of 13,578 genes in 31 amphibian species, including 10 aestivating species and 21 non-aestivating species. Based on the assumption that aestivation has two main requirements – a) metabolic regulation needed to control transitions to/from the hypometabolic state, and b) cell preservation strategies needed to sustain biological processes over long-term dormancy – we expected to find distinct relative evolutionary rates (RER) in genes related to those traits. We identified 323 genes with significant RERs; these genes were enriched for some processes overlapping with our predictions and with literature findings, such as shifts between glycolysis and oxidative phosphorylation. Other genes related to protein and membrane trafficking (TRAPP, SNARE, and Arp2/3 complexes) are newly associated with aestivation. RER patterns suggest that aestivation in amphibians relies on a set of highly conserved core processes and other auxiliary processes that have diversified across the phylogeny. Given the vast number and diversity of aestivating amphibian lineages, we predict that more in-depth molecular studies of amphibian aestivation will offer novel insight into hypometabolic processes that could inspire medical innovations to prevent organ atrophy, address problems with angiogenesis, and combat processes underlying cancer.

Introduction

Amphibians are distributed widely on Earth, except in regions with exceptionally limited access to liquid water such as the Sahara, Arabian, and Gobi deserts, or Antarctica (IUCN 2024, update 2023-1). These amazing vertebrates need humidity to survive, particularly because the vast majority carry out some gas exchange through their moist skin. Nevertheless, they have invaded and diversified in areas that might seem extreme, such as Central Australia or the Mojave and Sonoran deserts (Mayhew 1968). Amphibians living in seasonally arid environments avoid desiccation either by producing lipids that waterproof their skin (e.g., Amey and Grigg 1995; Jørgensen 1997) or by avoiding the hottest and driest season by resorting to aestivation, a physiological state in which they lower their metabolism and stay dormant for a lengthy period of time (weeks, months or even years), after which, when conditions are suitable, they raise their metabolism to continue daily activities (Navas and Carvalho 2010).

Aestivation is a preemptive state wherein animals prepare for water loss and diminished metabolic fuel supply. To avoid water loss, most amphibians seek refuge by burrowing. This does not mean that they resort to fossoriality because they are not active under the ground; rather they enter a state of depressed metabolism. Some amphibians while buried also produce cocoons made of multiple layers of shed skin, increasing the thickness of the cocoon according to the dryness of the environment (Booth 2006; Cartledge et al. 2006). The waterproof properties of the cocoon have been associated with the production of certain hydrophobic proteins such as ceramides and cerebrosides (Sadowski-Fugitt et al. 2012). Water loss is also retarded by colligative means, this implies elevating the osmolality of body fluids via the production of high concentrations of solutes like urea (a waste product of protein catabolism), in species that do not produce cocoons (Storey 2002; Luu et al. 2021). For example, spadefoot toads (*Scaphiopus*

couchii) do not produce cocoons, but urea can rise up to 300 mM in their blood after several months of estivation (McClanahan 1972). Moreover, it has been shown that water level does not change across tissues when aestivating compared to non-aestivating frogs (Bayomy et al. 2002).

Aestivation must be prefaced by the accumulation of large reserves of endogenous fuels to deal with starvation during the dormant period (Storey 2002), followed by a reduction in energy use during dormancy through a lower metabolic rate. A typical metabolic rate during estivation is approximately 10–30% of the corresponding resting metabolic rate in active individuals at the same temperature (Pinder et al. 1992). There are some extreme cases where, for example, *S. couchii* may reduce their resting metabolic rate 50% (Seymour 1973) or *Neobatrachus kunapalari* that can reduce it by up to 67% (Flanigan and Guppy 1997). It is also important to emphasize that the greater the reduction in metabolic rate, the longer the time that a fixed reserve of fuel can sustain basal metabolism, and the lower the amount of reactive oxygen species produced. It might be the reason why some amphibians seek hypoxic environments to accelerate entry into or deepen the hypometabolic state, for example *Rana amurensis* is capable of overwintering in water bodies under anoxic conditions using anaerobic metabolism (Berman et al. 2019). Food ingestion ceases and the digestive tract is substantially reduced in size (Akat et al. 2014; Cramp et al. 2005,2009). Energy metabolism during aestivation is based primarily on the anaerobic oxidation of lipids, although there seems to be some protein catabolism and a small direct contribution from carbohydrates. For example, in *Spea multiplicata*, the contributions to the total energy while aestivating were calculated as 62% from lipids, 32% from protein, and 5% from carbohydrate (Jones 1980). Protein synthesis, one of the most energy-expensive functions of cells, is strongly suppressed in estivating animals (Storey and Storey 2004,2010). For example, in liver slices from aestivating frogs in Australia, *Neobatrachus sudellae*, protein

synthesis was reduced by 67% compared with the rate in slices from non-aestivating frogs (Fuery et al. 1998). Furthermore, mechanisms of metabolic suppression in aestivators must be (a) rapidly reversible, and (b) require very little *de novo* protein synthesis and reorganization of metabolism, in order to both preserve energy and be prepared to enter into an active state as quickly as possible (Storey 2002; Storey and Storey 2012).

Aestivation may be an ancestral state in amphibians that has subsequently been lost many times in lineages where, presumably, aestivation is not necessary for survival (Ochoa-Ochoa et al. 2025). Here we take advantage of newly available annotated reference genomes to compare evolutionary rates of more than 13,000 genes between 10 aestivating species and 21 non-aestivating species. In this study we aim to: 1) identify candidate genes and biological processes that underlie estivation in amphibians, 2) evaluate whether these processes are highly conserved or derived in aestivating amphibians, and 3) review whether the genes we identify have been previously studied in amphibians or are newly identified. We employ an untargeted approach, which has the advantage of discovering potentially novel genes and pathways involved in this amazing adaptation.

Methods

Literature review

We followed a process similar to Ochoa-Ochoa et al. (2025) that consisted of performing a systematic search using the advanced search tool of each of the following search engines: Scopus, PubMed, and Web of Science, until December 2024. We used the words (aestivat* AND amphibian*) and (estivat* AND amphibian*). Studies were selected according to the following criteria: 1) empirical papers and reviews including theses; 2) empirical articles in which some biological, ecological, physiological, or genetic aspect of the aestivation process were mentioned; and 3) papers where the focus was not related to dormancy processes, but an aestivating species is mentioned. Afterwards we selected all the papers that contained the word "gene". Each of those published manuscripts was manually reviewed for a gene or protein involved in the aestivation process. Scientific names of amphibian species follow AmphibiaWeb (2024) nomenclature.

We recorded the tissue analyzed in each study (brain, heart, kidney, liver, muscle, lung, gut, and skin) because the same gene, miRNA, or metabolite can have increased activity in one tissue and decreased activity in another. In some manuscripts, skin and muscle were divided (e.g., dorsal and ventral skin), but here we considered these data together, without intra divisions. We also registered whether the activity was significantly increased or decreased in each tissue, and in the case of a non-significant change it was recorded as maintained. Thus, a single gene can be in both increased and decreased datasets. Due to the fact that some manuscripts did not report gene symbols, we used either the name of the gene provided or its description to search for gene symbols based on the *X. tropicalis* ensembl dataset (Dyer et al. 2025).

Obtaining sequence data

We initially attempted to use Orthofinder v2.5.5 (Emms and Kelly 2019) to identify orthologs across amphibian genomes, but the pipeline using primary transcripts identified only 161 single-copy orthologous genes. Reviewing the estimated gene duplications output from Orthofinder, three species were estimated to have a large number of duplicated genes: *X. laevis* (19,899), *Pelobates cultripes* (26,583) and *Staurois parvus* (66,924). Although it makes sense that *X. laevis* has so many duplications, as it is a tetraploid (Hughes and Hughes 1993), the other two species are thought to be diploid (Liedtke et al. 2022; Uno 2021). Both of these genomes were annotated by third parties. Although *Hymenochirus boettgeri* was also annotated by a third party, it did not show an inflated number of estimated gene duplications (8,452). After removing *X. laevis*, *P. cultripes*, and *S. parvus* from the Orthofinder analysis, we were still only able to identify 1,845 single-copy orthologs. Thus, we chose to develop a different pipeline based on NCBI gene annotations (see Supplementary Material Appendix A1, available online). We note that there are drawbacks to both of these methods, and neither is perfect. However, we believe that using the pipeline described below is adequate for the purpose of this study.

To get orthologs for amphibian genomes, we first downloaded the full gene set from *X. tropicalis* using the "datasets download gene taxon" command from the NCBI Datasets command line tools (O'Leary et al. 2024). Then we used a custom script (see Appendix A1, available online) to obtain and filter the metadata for gene names and symbols. The list of gene symbols was used to download all orthologs in amphibians using the "datasets download gene symbol" tool in NCBI Datasets. In some cases, multiple isoforms were available for an ortholog; thus, we selected the longest isoform for downstream analyses using a custom script. Once we had all ortholog sequences, we estimated sequence alignments for each gene using MAFFT

v7.526 (Katoh and Standley 2013) and gene trees using IQ-TREE v2.4.0 (Minh et al. 2020). Because downstream RER analyses require that the trees have the same topology, we used a tree from Portik et al. (2023) pruned to the species of interest to constrain the tree inference (option -g in IQ-TREE). *Microcaecilia unicolor* was not present in that tree, so we added the tip manually into the newick file. To adjust branching times for the caecilian clade including *M. unicolor*, we integrated estimates from TimeTree.org (Kumar et al. 2022): age of *M. unicolor* + *G. seraphini* = 120.1 MY; age of *M. unicolor* + *G. seraphini* + *R. bivittatum* = 221.3 MY. Finally, we rerooted the trees to standardize the topology using the root and reroot commands in ape v5.8-1 (Paradis and Schliep 2019) and phytools v2.4-4 (Revell 2024). All of the commands to obtain, align, and infer phylogenies of orthologs can be found in Appendix A1 (available online).

Estimation of evolutionary rates

We estimated the relative evolutionary rates of 13,578 genes based on *X. tropicali*s orthologs. In order to do so we used the RERconverge (Chikina et al. 2025) in R v. 4.4.2 (R Core Team 2024) to identify genes with consistent and significant departures from average rates of evolution across a phylogeny. Here we compare evolutionary rate in aestivating species to rates in putatively non-estivating species using binary trait data (species that aestivate = 1, species without info = 0). Of the 31 amphibian species with annotated genomes, ten are recognized to aestivate based on our literature review (Table 1, Figure 1).

We followed the developers' recommendations: no master tree provided and re-estimation of branch lengths when reading the trees; and for the function getAllResiduals we chose square root transformation, to use weighted regression for relative rates, and to scale

relative rates internally for each species subset (see Supplementary Material Appendix A2, available online). We developed three hypotheses:

H0 There is no set of genes with significant evolutionary rates associated specifically with aestivation.

H1 Only genes with significantly higher evolutionary rates (i.e., positive selection) are associated with aestivation which would imply diversification of the aestivation phenotype.

H2 Only genes with significantly lower evolutionary rates (i.e., purifying selection) are associated with aestivation which would imply conservation of the aestivation phenotype.

H3 Both genes with higher evolutionary rates and genes with low evolutionary rates are associated with aestivation, which would imply conservation of some aspects and diversification of others.

Finally, we compared gene symbols between significant RER genes and genes previously studied in our literature review to identify genes present in both datasets. We note that RER provides information on coding sequence evolution while most prior studies of aestivation have focused on gene expression, so we expected some overlap but note that the analyses provide different types of data.

Gene ontology analysis (GO analyses)

We performed a GO analysis on the genes identified by RER to be evolving at significantly different evolutionary rates in aestivating species. We used as background the set of genes that were estimated to have a Rho value, i.e., any gene with a positive or negative evolutionary rate regardless of the significance. In other words, we excluded the genes that have either a missing

(NA) or 0 value for Rho. Thus, we had a background dataset containing 13,183 genes, of which 323 had significantly accelerated (positive) or decelerated (negative) evolutionary rates; based on those genes we performed two GO analyses, one for positive and one for negative genes. It is important to specify that there is no overlap between the positive and negative datasets, since a gene has either a positive or negative Rho value.

We used the package *topGo* v2.58.0 (Alexa and Rahnenführer 2024) in R v4.4.2 (R Core Team 2024) to identify significantly enriched terms in our set of 165 / 158 (positive / negative) genes obtained from the RER analysis. For the gene2GO list of gene names and GoTerm identifiers, we used the annotated list for *X. tropicalis* (Bateman et al. 2025, https://www.uniprot.org/; downloaded June 12, 2025) that contains 76,381 entries. We used a nodeSize of 10 and for the significant genes and terms we set the topNodes at 50 (full script and data can be found in the Supplementary Material Appendix A3, available online).

We used Revigo (Supek et al. 2011) to simplify the visualization of GO terms through network inference and Cytoscape (Shannon et al. 2003) to visualize the networks. Finally, we searched for the protein name and function of the significant genes (https://www.uniprot.org/; accessed June 18, 2025) and significant terms (https://www.ebi.ac.uk/QuickGO/; accessed June 18, 2025).

STRING (Search Tool for the Retrieval of Interacting Genes/Proteins)

To further visualize results from RER, we input the significant positive and negative gene sets into the Search Tool for the Retrieval of Interacting Genes/Proteins (STRING) webtool (Szklarczyk et al. 2023). We estimated full networks (both functional and physical associations) using either *Homo sapiens* or *X. tropicalis* annotation information. We set the maximum number

of 1st shell interactors to 10, the maximum number of 2nd shell interactors to 5, the confidence to high (0.700), and hid disconnected nodes from the results. Shell interactors are proteins that are not in the query dataset but are predicted to interact with query proteins; including some of these in cluster inference assists the program in identifying protein complexes that may be relevant to the query dataset. Then we inferred gene network clusters using MCL clustering and default settings (with inflation parameter = 3). Results from *H. sapiens* were qualitatively similar to those from *X. tropicalis* and included slightly more annotations, so we only present networks from *H. sapiens.* However, when clusters were annotated using *X. tropicalis* data but not *H. sapiens*, we include this information clearly marked in the network.

Results

Literature review

From the 291 manuscripts found by Ochoa-Ochoa et al. (2025), 251 manuscripts contained the word gene, and of these, 39 contained information about a gene, metabolite, miRNA, or protein analyzed during aestivation or water restriction, i.e., dehydration (Table S1, Supplementary Material, available online). Some form of metabolic function or gene expression has been analyzed in 20 species, with *X. laevis* being the most common species, used in 15 studies, followed by *Cyclorana alboguttata* with 7 studies and *S. couchii* with 6. Studies have focused on different measurements of metabolic depression such as protein quantification (e.g., Bayomy et al. 2002; Luu et al. 2020,2018; Madelaire et al. 2020; Malik and Storey 2009; Malik et al. 2023; Pakay et al. 2003; Wu et al. 2017; Zhang et al. 2018), enzyme or metabolite activity (e.g., Bayomy et al. 2002; Cartledge et al. 2006; Flanigan et al. 1990; Katzenback et al. 2014; Patnaik and Sahoo 2021), miRNA abundance (e.g., Biggar et al. 2022; Luu and Storey 2015; Naranjo et

al. 2023), targeted RT-qPCR (e.g., Biggar et al. 2022; Luu and Storey 2015; Naranjo et al. 2023; Wu et al. 2013) and untargeted RNAseq (Reilly et al. 2013; Hudson et al. 2024 both with *X. laevis*).

1464 unique proteins, metabolites, and genes have been studied, as well as 74 miRNAs. Because they are not directly comparable to our results, which focus on genes that code for proteins, we exclude metabolites such as ATP, hormones or other compounds such as vasopressin, and miRNAs from further consideration (see full list in Table S2, Supplementary Material, available online). It is worth pointing out that of the >2500 genes showing significant changes in expression by Hudson et al. (2024), 739 sequences were not annotated (no BLAST results in their paper), and another 660 were not assigned a gene symbol through the search using the accession numbers provided; therefore, 1399 of their genes could not be included in our assessment. From the total 1434 genes/proteins with gene symbols, 707 had an increased activity and 755 had a decreased activity in at least one tissue. Skeletal muscle was the tissue most frequently analyzed followed by liver and kidney (Table S1).

Probably the most amazing aspect of aestivation that has been demonstrated is that although there is an overall metabolic depression, usually measured by O_2 consumption, there is a wide range in responses among tissues from no changes generally in the brain (e.g., Chauvet et al. 1993; Flanigan et al. 1990; Flanigan and Guppy 1997; Borah et al. 2020; Luu and Storey 2015; Wu et al. 2017,2020; Cowan et al. 2000) to extreme changes in the skeletal muscle (33 of the 39 articles mentioned found a significant change in muscle, Table S1). Of course, there are exceptions, for example, in aestivating *S. couchii* toads the brain contained increased activities of fructose-1,6-bisphosphatase (FBPase), phosphoenolpyruvate carboxykinase (PEPCK) and malic enzyme (ME), which all have roles to play in gluconeogenesis; it also had an increased activity

of b-Hydroxybutyrate dehydrogenase (BDH) suggesting the possible enhanced use of ketone bodies as an aerobic fuel for the brain (Cowan et al. 2000).

Estimation of evolutionary rates

We obtained orthologs for 31 species (Figure 1; Table 1), but for the analyses the maximum number of species in a single gene tree was 25. From this set of species only 10 have been recorded to aestivate according to the literature (*Bufo bufo, Bufotes viridis, Rana catesbeiana, Pyxicephalus adspersus, Pelobates cultripes, P. fuscus, Spea bombifrons, X. laevis, X. tropicalis,* and *Pleurodeles waltl*). RER results from 13,578 genes indicated 13,184 with Rho values, 394 without (when few sequences were available), 6,918 with an accelerated evolutionary rate (a positive Rho) and 6,265 with a negative Rho, thus indicating a decelerated evolutionary rate. In total, 165 had a significantly positive RER and 158 had a significantly negative RER, prior to multiple testing correction. When using the Benjamini-Hochberg correction (i.e., an estimate of the false discovery rate), no genes reached significance (full list can be found in Table S3 of the Supplementary Material, available online). The top ten genes ranked by p-values from accelerated (Table 2) and decelerated (Table 3) RERs showed diverse functions that in some cases were represented by significant terms in the GO analyses or were present in protein complexes inferred by STRING.

We found 1215 genes that overlapped between the 13,184 *X. tropicali*s orthologs and the 1434 genes identified in the literature review (Table S1). Of these 1215 genes, 30 also showed a significant RER in our analyses: 11 accelerated, and 19 decelerated. Of these 30, 9 showed increased activity in at least one tissue, and 18 showed decreased activity in at least one tissue;

lastly 3 showed increased activity in one tissue and decreased in another (GPI, JCHAIN, and PKM) (Table 4).

Gene ontology analysis

We identified a total of 148 significantly enriched terms when comparing genes identified with a distinct relative evolution rate (RER) to all genes in the background dataset ($p < 0.05$). 80 terms were significantly enriched in the RER accelerated gene set compared to the background gene set ($p < 0.05$). For the RER decelerated gene set, 68 terms were significantly enriched (Table S4, Supplementary Material, available online). Many genes were annotated with multiple terms (Fig. S1, in appendix A4, of the Supplementary Material, available online). Specifically, the terms correspond to 73 and 43 genes, respectively, for accelerated and decelerated evolutionary datasets, annotated to different GO term categories: 23 Molecular Function (MF), 71 Biological Process (BP) and 18 Cellular Compartment (CC) for accelerated and 26 MF, 18 BP and 17 CC for decelerated, respectively. Revigo summarized topGo results by collapsing similar terms into 64 parental terms, 22 for accelerated RER and 42 for decelerated RER.

MF showed 21 parental terms, 9 accelerated and 13 decelerated (Fig. S2, in appendix A4, available online). Accelerated terms, such as “protein-containing complex binding”, “phospholipid binding”, “lipid binding” and “NADP binding” are involved in intracellular trafficking, transport between the trans-Golgi network and endosomes. This is a pathway that promotes the recycling or degradation of internalized transmembrane proteins, it may also involve macropinocytosis which is a form of endocytosis that results in the internalization of extracellular content (Kay 2021). There are also various terms, such as “phosphatidylinositol phospholipase C activity” and “protein kinase inhibitor activity”, that are involved in the

transcription machinery particularly as regulatory and inhibitory processes. The decelerated terms, like “translation factor activity, “RNA binding”, “[DNA-directed 5'-3'] RNA polymerase activity”, and “catalytic activity, acting on a tRNA / RNA” are involved in transcription, ribosome and structural molecule activity related to protein synthesis and degradation of different polypeptides by substrate binding (e.g., “structural constituent of ribosome” and “structural molecule activity”).

BP had the largest number of parental terms after collapsing, 22 accelerated and 13 decelerated (Fig. S3, in appendix A4, available online). It is probably the most complex of all ontologies. Accelerated terms, such as “monosaccharide metabolic process”, “transcription by RNA polymerase III”, “nucleoside phosphate metabolic process”, “phosphorus metabolic process”, “glycosylation”, “pyridine-containing compound metabolic process”, “macroautophagy”, “carbohydrate derivative metabolic process”, and “carbohydrate derivative biosynthetic process”, are involved in the pentose phosphate pathway (PPP) for carbohydrate degradation, an alternative to glycolysis and a major source of reducing power and metabolic intermediates for biosynthetic processes; others such as “vesicle-mediated transport”, “macromolecule localization”, “intracellular transport”, “Golgi vesicle transport” and “cellular localization”, are involved in intracellular and endosomal membrane trafficking and in transport between endoplasmic reticulum and the trans-Golgi network (TGN). The term “cellular process” was the most complex and presented the highest number of genes involved, 70 in total. The decelerated terms, like “purine ribonucleotide metabolic process”, “cyclic nucleotide metabolic process”, “cyclic nucleotide biosynthetic process”, “ribose phosphate metabolic process”, “translation”, “amino acid activation”, and “tRNA aminoacylation for protein translation”, are

involved in translation, in the formation of cAMP in response to calcium entry leading to cAMP signaling activation, and in glycolysis.

CC had the smallest number of parental terms after collapsing, 3 accelerated and 3 decelerated (Fig. S4, in appendix A4, available online). The accelerated terms ("endoplasmic reticulum protein-containing complex", "organelle subcompartment" and "perinuclear region of cytoplasm") are involved in the retrograde transport from endosome to plasma membrane, a trafficking pathway that promotes the recycling of internalized transmembrane proteins. It also mediates delivery of transmembrane proteins into the lumen of the lysosome for degradation. The decelerated terms, like "mitochondrial inner membrane", "mitochondrion", "ribosome" and "perinuclear region of cytoplasm", are involved with the protein synthesis and the ribosome which is a large ribonucleoprotein complex responsible for the synthesis of proteins in the cell.

STRING (Search Tool for the Retrieval of Interacting Genes/Proteins) Results

STRING MCL clustering inferred 17 clusters for the accelerated gene set and 20 clusters for the decelerated gene set (full list can be found in appendix A5 of the Supplementary Material, available online). The largest cluster in the accelerated gene set (Fig. 2) was the TRAPP complex (10 genes, although 8 are inferred interactors), followed by an unnamed cluster with 6 genes (1 inferred interactor) possibly related to translation deduced by the involved genes (SRPRA, RPL37, RPS26, GSPT1, BTF3, TMCO1), a cluster of 4 genes (1 inferred interactor) related to glucose 6-phosphate metabolism, an unnamed cluster of 3 genes related to angiogenesis (CDIPT, NOS3, PLCG1), a 3-gene cluster related to endosome trafficking (labeled PhoX homologous domain), among others. In the decelerated gene set (Fig. 3), the largest cluster was oxidative phosphorylation (25 genes, 9 of which are inferred interactors), followed by mitochondrial

translation (10 genes, 1 inferred interactor), regulation of renal output by angiotensin (4 genes), an unnamed cluster (3 genes) related to purine metabolism (NPR2, PKM, RRM2), a 3-gene cluster related to RNA polymerase (though labeled as “Abortive elongation of HIV-1 transcript in the absence of Tat”), an unnamed 3-gene cluster related to ribosomes, among others.

Discussion

In order to respond quickly and appropriately to a stressful environment, organisms can change gene expression, as it underlies virtually all cellular responses to external stress and readjusts the protein content, and therefore the function of the cell. It has been suggested that a hypometabolic state can occur with gene expression changes in only a subset of processes that are key for survival (Storey 2000), such as conservation of energy via two pathways switching to lipid fuel and protein metabolism. Yet, the number of genes that respond during hypometabolism is impressive, as Hudson et al. (2024) observed more than 2500 significantly upregulated or downregulated genes in the skeletal muscle of aestivating frogs (*Cyclorana alboguttata*). This demonstrates that entry into a hypometabolic state requires responses by a huge variety of cell functions (Storey and Storey 2007). Prior studies of aestivation in amphibians have focused on changes in gene expression and resulting fluctuations in metabolites or enzyme activity, and most studies have targeted specific processes or genes, such as protein phosphorylation, glycolysis, and the activity of specific transcription factors. In contrast, we take an untargeted approach and use signatures of selection (quantified by significantly altered evolutionary rates) to identify genes putatively involved in aestivation in amphibians. By doing so, we are not only able to add novel lines of evidence supporting the role of some processes already known to be involved in aestivation, but we can also identify new genes and processes that might underlie

hypometabolic states. Here we first review the general themes apparent in our results. Then we revisit our hypotheses and discuss what the different evolutionary signatures we observe can tell us about the aestivation phenotype. Finally, we compare our results to what was previously known to identify how our study contributes to the field.

Shifts in energy use and production

Two of the main pathways used to produce ATP in cells are anaerobic glycolysis and oxidative phosphorylation. In aestivating amphibians, aerobic energy production via oxidative phosphorylation is limited due the oxygen limitation in tissues. Therefore, metabolic ATP production shifts from oxidative phosphorylation to anaerobic production of ATP, where pyruvate is converted to lactate to regenerate the NAD+ needed to sustain glycolysis (Dawson et al. 2018). Lactate dehydrogenase (LDH) is responsible for catalyzing the reversible reaction of pyruvate and NADH to lactate and NAD+. Much of the prior research has focused on genes and regulatory mechanisms that are involved in either of these pathways (more than 20 articles). For example, Katzenback et al. (2014) found differences in kinetics, post-translational modifications, and stabilities of LDH, they also found that its function is maintained at elevated urea levels (150 mM) under dehydration stress in *X. laevis.*

It is now known that reversible phosphorylation control of pyruvate kinase (PK) is one way of regulating the aerobic versus anaerobic energetic pathways present in many species of animals, from aestivating snails to hibernating small mammals (Storey & Storey 1990; Storey 1997; Brooks & Storey 1997; Cowan & Storey 1998). As an example, Dawson et al. (2018) showed increased function of PK during severe dehydration in aestivating *X. laevis* compared to control frogs. Regulation of PK activity occurs via multiple mechanisms, including tight

allosteric regulation and regulation via insulin-mediated cell signaling pathways (Wu et al., 2017). According to our RER results, PKM, the gene for muscle PK in *X. tropicalis*, has a significantly decelerated RER, implying that the gene has been conserved. As the action of PK seems to be crucial to deal with dehydration, and we see little change in the coding sequence in aestivating species, either the function of the protein is similar to the ancestral state or its function has been modified through other routes such as phosphorylation and gene expression changes (e.g., Luu et al. 2020; Madelaire et al. 2020; Malik and Storey 2009; Pakay et al. 2003; Wu et al. 2017,2020; Zhang et al. 2018).

Our results further support the importance of energy pathways in aestivating amphibians, as the largest gene cluster identified by STRING in either data set was oxidative phosphorylation (Fig. 3, decelerated). STRING also identified two unnamed clusters (3 genes, 2 genes) related to purine metabolism (including GPI and PKM, critical to glycolysis), as well as two genes related to fatty-acid metabolism ("malonyl-CoA metabolism") in the decelerated data set (Fig. 2). GPI and PKM have been studied previously; as mentioned above, the latter was upregulated in severely dehydrated *X. laevis* (Dawson et al., 2018). Both Reilly et al. (2013) and Hudson et al. (2024) found downregulation for PKM and for GPI, whose product is Glucose-6-phosphate isomerase, which is crucial in the inhibition of glycolysis. GPI was also shown to increase prior to hibernation in the Chinese brown frog (*Rana dybowskii*) (Fan et al. 2022) and elevate during hibernation in the brown bear (*U. arctos*) (Chazarin et al. 2019a). In the accelerated gene set, STRING identified a cluster of genes related to glucose 6-phosphate metabolism (Fig. 3). GO term analyses identified several enriched biological processes related to these pathways including fatty acid and carbohydrate biosynthesis processes as well as and ribose phosphate, cyclic nucleotide, and purine ribonucleotide metabolic processes in the decelerated data set and

carbohydrate derivative, nucleoside phosphate, pyridine-containing compound, and monosaccharide metabolic processes enriched in the accelerated dataset. Pyridine-containing compound metabolic processes includes NAD+ catabolism, resulting in NADH, and NAXE, present in the decelerated dataset, helps keep NADH supplies in the correct format (Manor et al. 2022).

When sufficient NADH and oxygen are available, oxidative phosphorylation is carried out in the mitochondria via five protein complexes, producing relatively large quantities of ATP. Several members of each complex were represented in the decelerated gene set, and none were present in the accelerated gene set, suggesting strong evolutionary conservation of this process: TIMMDC1, NDUFB1, NDUFB2, NDUFB3 (a top-ten RER; Table 3), NDUFB7, NDUFB8, NDUFC1, NDUFS4, NDUFV3 in Complex I; DMAC2 in Complex II; UQCR11 and UQCRQ in Complex III; COA3, COX6C, and COX7A2 in Complex IV; ATP5F1A (another top-ten RER; Table 3), ATP5PB, ATP23, and ATP5PD in complex V. In estivating *C. alboguttata*, the expression of NDUFB3, NDUFS4, ATP5PB, and other related proteins are all downregulated, as part of a global repression of ATP production concomitant with a lower need for energy in the aestivating state (Hudson et al. 2024). The mitochondrion itself was an enriched cellular component (Fig. S4). MICOS13, present in the decelerated gene set, is related to the formation of cristae in the mitochondria, which is directly related to its oxidative phosphorylation capacity (Khosravi and Harner 2020). This strong evolutionary conservation might be related to the brief period of activity that most amphibians living in extreme environments have, therefore they have to be absolutely efficient in renewing their energetic reserves.

Many of the genes that are involved in glycolysis change in expression during dormancy (aestivation and hibernation) and hypoxia in other animals, not only in amphibians. The role of

G6PD, glucose-6-phosphate dehydrogenase, which hydrolyzes glucose-6-phosphate into a glucose and phosphate group in the PPP, represents a route for the breakdown of carbohydrates besides glycolysis. G6PD has increased activity in the brain and skeletal muscle (but decreased activity in the liver) of aestivating *S. couchii* toads (Cowan et al., 2000), and reduced activity in hibernating squirrels (*Spermophilus parryi*) (Smullin & Behrisch, 1981) and diapausing flesh fly pupae (*Sarcophaga crassipalpis*) (Chen et al., 2020). ACACA, present in our decelerated gene set, is involved in fatty acid synthesis and has been found to have reduced expression in hibernating grizzly bears (*Ursus arctos horribilis*), black bears (*U. americanus*), Himalayan marmots (*Marmota himalayana*), and tree shrews (*Tupaia belangeri*) (Jansen et al. 2019; Fedorov et al. 2025; Bai et al. 2019; Hou et al. 2023). HK1, present in our accelerated gene set and involved in glycolysis, has been shown to have increased expression in the skeletal muscle during aestivation in *C. alboguttata* (Hudson et al. 2024), during anoxia in *Trachemys scripta* turtles (KennethSparks et al. 2021) and *Rattus norvegicus* rats (Waskova-Arnostova et al. 2015), as well as during dormancy in *Apostichopus japonicus* sea cucumbers, and in *Microcebus murinus* mouse lemurs during torpor (Biggar et al. 2015; Yang et al. 2021). However, HK1 expression decreased in hibernating grizzly bears (*U. a. horribilis*) and in Horseshoe bats (*Rhinolophus ferrumequinum*) during torpor (Jansen et al. 2019; Xiao et al. 2015), suggesting some variation in the role of glycolysis among species during dormancy. In addition, during dormancy, some organisms transcribe but do not translate certain genes, or pause the glycolysis pathway at later steps, to build up reserves of intermediates that can be accessed immediately upon awakening (Hudson et al. 2024).

Enhancement of antioxidant defenses is proving to be a universal feature of hypometabolism across distant lineages of life (Storey and Storey 2007). In aestivating

amphibians, enzymatic and metabolite antioxidant defenses are adaptable systems that can be easily modified in response to stressful conditions (i.e., hot and dry environments) in order to enter a hypometabolic state as well as to exit it when conditions return to suitable conditions (Grundy & Storey, 1998). One antioxidant gene was present in the gene set: ATOX1. In contrast, NOS3, which produces nitrous oxide, a source of reactive oxygen species (ROS) (Canty, 2000), was present in the accelerated gene set and was one of the most significant RER genes (Table 2). NOS3 was previously found to be downregulated in skeletal muscle in *C. alboguttata* (Reilly et al. 2013). Several genes involved in DNA repair, including FAM168A (decelerated), and SIRT7, SSRP1 and YBX1 (accelerated) were present in our dataset (Fig. 4). Expression of YBX1 was found to be downregulated in aestivating *C. alboguttata* (Hudson et al. 2024). In aestivating amphibians, Glucose-6-phosphate dehydrogenase (G6PDH) promotes carbohydrate entry into the PPP to produce sugar phosphates for biosynthesis producing reduced forms of glutathione and thioredoxin by NADPH reducing power to drive antioxidant defense. This reducing power is crucial to prevent and minimize oxidative damage to macromolecules during dormancy. Although G6PDH was not present in our significant RER gene sets, G6PDH activity has been shown to be increased during aestivation in *S. couchii* and *Rana pipiens* (Cowan et al. 2000; Cowan and Storey 2002). Increased G6PDH activity during oxidative stress is also present in other species such as land snails (*Otala lactea*), marine mollusks (*Littorina littorea*) and in wood frogs (*R. sylvatica*) (Hermes-Lima et al. 2015; Giraud-Billoud et al. 2024). Complementarily, inhibited and/or reduced G6PDH activity has been correlated with reduced antioxidant capacities, even death (Navas and Carvalho 2010). Notably we didn’t find NRF2 or any FOXO genes in our RER significant datasets, which are canonical responses to ROS (Giraud-Billoud et al. 2024; Malik and Storey 2009,2011).

Transcription and translation are central targets of selection in aestivating amphibians

Transcription and translation are energetically costly, and during dormancy, animals often reduce these processes to both save energy and avoid generating products that are not in high demand (Storey and Storey 2007; Hawkins and Storey 2020). One way that transcription can be reduced is by increasing methylation or decreasing acetylation of histones; this reduces the accessibility of DNA to transcription factors and ultimately reduces transcription rates (Jiang et al. 2023). STRING identified two members of the Sin3 complex (SAP30 and SUDS3) involved in histone deacetylation in the accelerated gene set, whose activity would make chromatin more tightly packed and less accessible for transcription (Wang et al. 2023). Although histone modification was not identified as an enriched process (e.g., the GO terms ubiquitin-modified histone reader activity, histone binding, or histone deubiquitinase activity are not enriched in our datasets), there were a number of additional genes related to histone binding and accessibility present in the accelerated dataset including AUTS2, BRD9 (top ten RER; Table 2), EYA4, KDM5B, SIRT7, SSRP1, and YEATS2 and in the decelerated dataset, including CTCF, NCOA3, NLK, RYBP (Fig. 4). KDM5B, a histone demethylase, has been shown to have decreased expression in wood frogs (*R. sylvatica*) during freezing (Taiwo et al. 2024). In addition, two of these genes (AUTS2, RYBP) are members of the Polycomb group (PcG) proteins, which are a conserved family of epigenetic regulators of gene expression. In the central bearded dragon (*Pogona vitticeps*), PcG plays an important role during hibernation by repressing transcription (Capraro et al. 2019). SAP30 and AUTS2 were both downregulated in aestivating *C. alboguttata* (Hudson et al. 2024).

In reviewing the GO term and STRING results, we noted that many other genes and processes integral to transcription and translation were identified to be enriched in the RER gene sets (Fig. 4; Figs. S2–S4). For example, “transcription by RNA polymerase III” was a biological process enriched in the accelerated gene set (Fig. S3). Two genes encoding RNA polymerases present in the decelerated gene set were highlighted by STRING (POLR2B, POLR2K) along with SUPT5H, which is implicated in transcription efficiency (Naguib et al. 2019). POLR2B is downregulated in the skeletal muscle in aestivating *C. alboguttata* (Hudson et al. 2024). In estivating snails (*Bostryx conspersus*), the expression of RNA polymerases was downregulated (Pourazami 2024). Many transcription factors and proteins related to transcription factor function were also present in the accelerated gene set, including CALCOCO1, CDK7, COMMD7, DRGX, HEXIM1, MED12, SCX, SNAPC5, SSRP1, and ZNF131; two were also present in the decelerated gene set (MED13 and RUNX3) (Fig. 4). At least two of these genes have been implicated in responses to hypoxia and hibernation in animals previously: HEXIM1 is upregulated in heart cells of lab mice (*Mus musculus*) following hypoxia, possibly helping to prevent hypertrophy (Yoshikawa et al. 2012); MED12 is upregulated during torpor in Himalayan marmots (*M. himalayana*) (Bai et al. 2019).

If produced, mRNA resulting from transcription can be temporarily hidden from translation machinery, for example by being reversibly bound by CPEB1 (decelerated), which is a mechanism that would allow the buildup of reserve mRNA that can later be translated when protein products are needed (Chengand Schuh 2024), while avoiding unnecessary energy expense during dormant periods. A few genes related to miRNA and RNA degradation were also present in both datasets, including DBR1, YBX, TARBP2, and WTIP (Fig. 4).

In contrast to the mixed patterns of selection on genes related to transcription, genes relating to translation were largely characterized by decelerated RERs. An impressive number of the components of the ribosome and mitoribosome were present in the decelerated gene set including MRPS2, MRPS5, MRPS9, MRPS25, MRPS28, MRPS35, RPL24, and RPL35A; two additional genes, RPS26 and RPL37 were present in the accelerated gene set (Fig. 4). Three genes involved in the assembly of the ribosome complex were also identified within the decelerated gene set (FCF1, GAR1, and RSL24D1). Although one may generally expect that translation machinery is under purifying selection, here we find that it is even more conserved in aestivating compared to non-estivating species. A number of genes related to tRNA function, as well as the initiation and termination of translation, were present, mostly in the decelerated gene set (Fig. 4; including MTRF1L, one of the top ten significantly decelerated RERs; Table 3). One of these genes, GUF1, helps promote mitochondrial protein synthesis under less-than-optimal conditions (Bauerschmitt et al. 2008). The GO terms “translation” and “amino acid activation”, related to amino acids being attached to their respective tRNA, were enriched in the decelerated gene set (Fig. S3), along with their corresponding cellular locations (ribosome, ribonucleoprotein complex, and mitochondrion; Fig. S4), and associated molecular functions including “catalytic activity, acting on RNA and tRNA”, and “structural constituent of ribosome” (Fig. S3). One of these decelerated genes, SARS1, had an increased expression in the skeletal muscle of *C. alboguttata* (Reilly et al. 2013). Finally, STRING identified two clusters of genes involved in translation in the decelerated gene set (“Mitochondrial translation,” “initiation factor;” Fig. 3). The expression of translation initiation factors has previously been shown to be altered during periods of dormancy in animals. For example, EIF4H (accelerated) is upregulated during torpor in tenrecs (*Tenrec ecaudatus*) (Khudyakov et al. 2021), EIF2S3 (decelerated) is downregulated

in aestivating snails (*Bostryx conspersus*) (Pourazami 2024), and EIF4ENIF1 (accelerated) is upregulated in the skeletal muscle in aestivating *C. alboguttata* (Hudson et al. 2024).

Possible signature of selection on membrane and protein trafficking

Another major biological process that was significantly enriched in our results was the transport of proteins and macromolecules (Fig. 4; Fig. S3). Metabolizing proteins and lipids from cell membranes or from cells undergoing apoptosis can both provide nutrients and allow animals to reconfigure their tissues for new environments (Hawkins and Storey 2020; Storey and Storey 2004). For example, removing aquaporins from cell membranes helps protect against desiccation in a killifish (*Fundulus heteroclitus*) (Tingaud-Sequeira et al. 2013). In yeast experiencing glucose starvation, cells halt membrane protein recycling, which results in an increased retention of membrane proteins for metabolism and ATP production (Lang et al. 2014). The possible importance of these processes in aestivating amphibians was made salient in STRING through the identification of several protein complexes involved in membrane fusion and transport processes. The TRAPP (TRAnsport Protein Particle) complex (represented by TRAPPC5 and TRAPPC6B, under accelerated RERs), is involved in docking and/or tethering vesicles to a target membrane (e.g., the ER or the Golgi apparatus) (Sacher et al. 2008). TRAPPC6B is the second most significant accelerated RER gene (Table 2). The SNARE complex (tSNARE, STXBP6, VPS18; all accelerated) helps fuse membranes together (Ungar and Hughson 2003). Sorting nexins (SNX5, SNX8, SNX10, and SNX27; all accelerated), highlighted by STRING as a “PhoX homologous domain” cluster, are involved in membrane trafficking and the endosome pathway (Cullen 2008). The Arp2/3 complex (ARPC3, ARPC5; both decelerated) is involved in forming branched actin, which is necessary to move endosomes (Rotty et al. 2013). Other

proteins involved in endocytosis were also present in our RER significant gene datasets, although they were not highlighted by GO or STRING: HIP1, AP1AR, WDR81, UNC119, and COMMD7 (all accelerated); RUFY1 (decelerated). Members of the exocyst complex were also present: RALGAPA2, SYNGR3, and VPS18 (all accelerated; VPS18 is a top-ten RER gene; Table 2); EXOC1 (decelerated). In general, there were many genes involved in protein and membrane trafficking in our significant gene sets, mostly under accelerated RERs (Fig. 4). A number of genes related to trafficking to the Golgi apparatus (ARF4, decelerated; ARF3, ERGIC1, AP1AR, all accelerated; Fig. 4), where proteins are subsequently modified and sent for degradation or to the cell membrane, were also present in the significant gene sets.

Related to these functions are the targeting and breakdown of proteins for energy, and/or as a response to ROS damage (see section above). The molecular function GO Terms "metallopeptidase activity" and "metalloendopeptidase activity" were enriched in the decelerated gene sets (Fig. S2). These are related to protein breakdown. Polyubiquitination involves tagging a protein with multiple ubiquitin molecules, often then leading to its degradation (Voet et al. 2008). Several ubiquitin enzymes were present in our dataset, including ubiquitin-conjugating enzymes (E2s) UBE2G1 and UBE2V2 (both decelerated), ubiquitin-protein ligases (E3s) SH3RF2, RAB40C (both accelerated), and RNF212B (decelerated), as well as proteins that can remove ubiquitin tags (YOD1, accelerated, and IDE, decelerated). STRING identified the two E2s as a cluster (Fig. 3) and the RER of UBE2G1 was the second most significant in the decelerated gene set (Table 3). Previously it was shown that UBE2G1 is upregulated during aestivation in green striped burrowing frog *C. alboguttata* (Hudson et al. 2024) and, more generally, that protein degradation was enriched during torpor in tenrecs (*T. ecaudatus*) (Khudyakov et al. 2021).

Autophagy is another mechanism to recycle nutrients (and reduce damage from ROS) by degrading internal organelles and molecules in endosomes. The biological process GO term "macroautophagy" was enriched in our accelerated RER gene set (Fig. S3). In total, more than 10 genes involved in autophagy were present in our datasets. Some of these are specifically related to lysosomes or peroxisomes (accelerated: ACBD5, YOD1; decelerated: PSAP), the formation of autophagosomes (accelerated: ATG2A, TBC1D25), or ER-phagy (TEX264; one of the most significant accelerated RER genes, Table 2). DDIT4, present in the decelerated gene set, has been shown to be downregulated in response to dehydration in skeletal muscle in *C. alboguttata* (Reilly et al. 2013), and to be related to autophagosomes (Ho et al. 2020). Membrane fusion is involved in autophagy, and as discussed above, several protein complexes involved in membrane fusion or trafficking were identified in our results.

At a larger scale, apoptosis can also contribute to nutrient metabolism, induced by cellular damage (e.g., through action by ROS), or through other physiological processes. Three genes with accelerated RERs are related to inhibition of apoptosis (BFAR, DAD1, MDM4; DAD1 is a top-ten RER) while two with decelerated RERs are related to the promotion of apoptosis (RUNX3, RYBP). In prior studies, BFAR was shown to be downregulated in the skeletal muscle in aestivating *C. alboguttata* (Hudson et al. 2024), and DAD1 was shown to be upregulated during torpor in *Myotis ricketti* bats (Huang et al. 2020) and in hibernating Himalayan marmots (*M. himalayana*) (Bai et al. 2019). A number of other genes with various roles related to homeostasis or indirect interactions with apoptosis genes were present in each gene set (accelerated: CDK7, GRAMD4, HIP1, NAIF1; decelerated: ANP32B, DKK1, DNAJA3, ERBB4, RPL35A). Previously, ANP32B was shown to be upregulated in the skeletal muscle in aestivating *C. alboguttata* (Hudson et al. 2024). Apoptosis-inducing factor 2 (AIFM2)

was the gene with the highest increase in expression in the skeletal muscle in aestivating *C. alboguttata* (Hudson et al. 2024). However, although AIFM2 presented a decelerated relative evolutionary rate in our study, it was not significant.

Other emerging themes

A few unexpected groups of genes were identified. For example, an unnamed cluster of 3 genes containing two related to angiogenesis (PLCG1, NOS3) was identified by STRING in the accelerated dataset (Fig. 2); similarly, STRING identified a cluster of 4 genes in the decelerated gene set related to the regulation of renal output by angiotensin (Fig. 3). One of these genes, ACE, angiotensin-converting enzyme, was previously identified to be downregulated in response to dehydration in skeletal muscle in *C. alboguttata* (Reilly et al. 2013; Hudson et al. 2024). ACE inhibitors are commonly used in patients with high blood pressure to block the activation of angiotensin and avoid the constriction of blood vessels and lower blood pressure; they can also cause angioedemas (Cutrell et al. 2023). In Syrian hamsters, decreased ACE activity is associated with maintenance of lung tissue during torpor (Talaei et al. 2012). In high-altitude Himalayan marmots (*M. himalayana*), it's been proposed that changes in the angiogenesis pathway can help avoid over proliferation of blood vessels in response to lower oxygen availability (Bai et al. 2019). The VEGFA-VEGFR2 signaling pathway, involved in angiogenesis, was overrepresented during torpor in tenrecs (*T. ecaudatus*) (Khudyakov et al. 2021). Aestivating amphibians need to respond to low oxygen availability by activating VEGF (to stimulate angiogenesis), however it is counter-intuitive to enhance capillary growth since the problem is not oxygen delivery but a lack of oxygen overall. Therefore, upregulation of pigment

epithelium-derived factor (PEDF) might counteract a VEGF-mediated angiogenic response in hypoxic environments (Storey and Storey 2007).

Genes involved in post-translational modifications were also common in our significant gene sets. Above we discuss ubiquitination, but glycosylation and phosphorylation were also common themes (Fig. 4). Glycosylation is a ubiquitous co- or post-translational protein modification process that affects protein solubility, stability, and function (Lauc and Wuhrer 2017). We identified several genes related to glycosylation in both our accelerated (B3GALT2, MOGS, ST3GAL2, ST3GAL4, TMTC2) and decelerated (GALNT16, RAMP1) gene sets (Fig. 4). Prior studies have shown that TMTC2 is possibly related to adaptation to high elevation in sheep and pika (Sjodin 2023; Yang et al. 2016). ST3GAL2 is downregulated in hibernating Daurian Ground Squirrels (*Spermophilus dauricus*), and glycosylation in general was identified as an important process in their ability to avoid muscle atrophy during hibernation (Dang et al. 2020). The GO terms “cellular process”, “glycosylation”, “carbohydrate derivative biosynthetic process”, and “carbohydrate derivative metabolic process” are related to these functions. Protein phosphorylation is another prevalent theme in our significant genes (Fig. 4), as well as prior studies of aestivation. We found a prevalence of kinases in our data set including several representatives of the cyclin-dependent kinases (accelerated: CCND1, CDKN1B; decelerated: CCNI2, CDK7). CDKN1B was found to be downregulated in response to dehydration in skeletal muscle in *C. alboguttata* (Reilly et al. 2013). Also, present were GPRC5B (top ten accelerated RER; Table 3), which modulates the NF-kB signaling pathway involved in responses to stress, resulting in downstream phosphorylation activity, and MYDGF (decelerated), which results in changes in phosphorylation through the MAPK signaling pathway (Luu et al. 2021).

Phosphatases, which remove phosphoryl groups from proteins, were not as prevalent in our data (only EYA4 and PXYLP1 were present in the accelerated dataset).

Genes related to cell cycle progression were overrepresented in our results. Specifically, in the accelerated gene set, several genes were related to the Wnt-signalling pathway, and the molecular function GO term “beta-catenin binding” was enriched. In addition, two genes in the decelerated gene set related to Wnt-signalling were identified by STRING in “RUNX3 regulates WNT signaling”. More than ten genes associated with cell cycle progression were present in our significant gene sets (accelerated: CCNI2, CDKN1B, GSPT1, HOXD10, MDM4, SCRIB, SIRT7; decelerated: ANP32B, CCND1, DDIT4, ERBB4, FANCD2, FGFR1OP, NCAPD2, NPR2, RRM2, RUNX3, UBE2V2, WTIP). It was previously shown that CDKN1B is upregulated in the testis of a cavefish (*Onychostoma macrolepis*) during torpor (Ma et al. 2024) and in killifish (*Nothobranchius furzeri*) during diapause (Hu et al., 2020) and in zebrafish (*Danio rerio*) under hypoxia (Jopling et al. 2012); its action is suggested to inhibit cell proliferation and promote muscle preservation (Ma et al. 2024). CDK7 and CDKN1B (also mentioned above) were identified as part of an unnamed gene cluster related to the cell cycle by STRING (Fig. 2). The role of cell cycle progression in aestivating amphibians could be two-fold: 1) limit tissue growth during aestivation and 2) promote rapid tissue growth during the awakening period prior to reproduction. More studies of genes involved in cell-cycle progression could help provide insight into mechanisms promoting or preventing the development of cancers. In general, cancer is a rare phenomenon in amphibians (Torres-Dimas et al. 2022; Compton et al. 2025).

Finally, we note several other groups of genes present in our data: homeobox genes, important for development (DRGX, EVX2, HHEX, HOXB2, HOXB9, HOXD10, NKX2-5; all

accelerated); genes involved in cell-cell adhesion or junctions (accelerated: CLDN11, CLDN7, DLG1, CLRN1, PARVA, TEX264; decelerated: ADAM23, CDHR3, DSCAM, GJB2, GJC1, MICOS13, WTIP), and a few genes involved in sperm function (all decelerated: MMEL1, SPACA6, SPATA6) or hormones (accelerated: GALP, GALR2, also highlighted by STRING in Fig. 2, and SCT; decelerated: ACE, IDE, NPR2). SCT is involved in mechanisms of satiation and homeostasis in regard to pH in the stomach (top 10; Table 2). In hibernating amphibians, galanin (encoded by GALP, binding to receptor GALR2) may be linked to shifts in metabolic fuel sources or decreased responses to stress (González Nicolini et al. 1998). A gap junction protein (GJB1) was found to be upregulated in hibernating thirteen-lined ground squirrels (*Ictidomys tridecemlineatus*) (Hampton et al. 2013) and muscle structure was a theme in gene expression changes in the skeletal muscle in aestivating *C. alboguttata (Reilly et al. 2013).* ADAM23 gene expression has been associated with cell-cell and cell-matrix interactions was also found to be downregulated in response to dehydration in skeletal muscle in *C. alboguttata* (Reilly et al. 2013; Hudson et al. 2024). Genes involved in sperm function and hormones may be related to the unique life histories of aestivating amphibians, which require rapid periods of reproduction following long aestivation periods (Shalan et al. 2004; Wilsterman et al. 2021).

Relative evolutionary rates of genes associated with aestivation; revisiting the hypotheses

We hypothesized that the selection patterns in our data would provide insight into both the mechanisms permitting aestivation as well as the evolutionary signatures associated with its origin and maintenance. Given that aestivation is thought to be an ancestral state of amphibians (Ochoa-Ochoa et al. 2025), we hypothesized (H1 & H3) that some genes would be highly conserved and show decelerated relative evolutionary rates (RERs). Yet, the ecological and

phylogenetic diversity of the amphibian species that aestivate may result in positive selection on some genes, diversifying their functions in accordance to species-specific ecological and physiological needs (H2 & H3). Parsing apart these patterns can provide insight into possible core and auxiliary mechanisms of the aestivation phenotype.

Most of the processes represented by genes in our results show a mixture of accelerated and decelerated rates, supporting H3 and demonstrating that the retained ancestral phenotype relies both on a core set of highly conserved processes and a set of auxiliary processes that have diversified with time. However, there are a few notable exceptions. First, the genes in our datasets that are related to oxidative phosphorylation and translation are all under decelerated RERs. The ubiquity of decelerated relative evolutionary rates in genes linked to these processes suggests that there has been especially strong negative selection on translation and oxidative phosphorylation in aestivating amphibians, and identifies them as a core conserved process in relation to aestivation. Having well-functioning machinery for oxidative phosphorylation and translation could be important both during aestivation, to preserve energy, and during active periods, to quickly recover, reproduce, and renew the energetic reserves (Vieira de Andrade et al. 2016). Nevertheless, these patterns suggest that among aestivating amphibians, it is beneficial or necessary for the genes underlying these processes to remain relatively unchanged from their ancestral sequences. We note that other processes, such as phosphorylation and epigenetic modifications could alter these processes without changing the coding sequences.

Two processes were predominantly under accelerated RERs: the homeobox genes and most of the genes involved in protein and membrane trafficking (Fig. 4). These patterns suggest that development and trafficking is diverse among aestivating amphibian lineages. We hypothesize that many of the genes related to the metabolism of cell membrane lipids and

proteins are under accelerated evolution in aestivating amphibians because of the variety of needs of and resources available to each species, necessitating different solutions to conserve energy and limit the increase of ROS (Jiang et al. 2023).

We note one additional intriguing pattern. The RERs of the three genes related to inhibition of apoptosis were all accelerated while that of the two genes related to the promotion of apoptosis were decelerated. If this pattern reflects the evolutionary history of selection on apoptosis, it suggests that in aestivating amphibians, the mechanisms promoting apoptosis are highly conserved while those inhibiting it are diverse. Finally, we want to note that a lack of significance after multiple testing correction as occurred here is fairly common in studies that use RER (Chikina et al. 2016), including in the tutorial outlined in the R package documentation (Kowalczyk et al. 2019; Meyer 2018). It is likely related to the large number of genes involved in these studies.

Comparison between our results and prior studies

In our literature review, we found a predominance of targeted studies (Table S1), which focus on a subset of genes, proteins, or metabolites putatively involved in the hypometabolic state, rather than untargeted studies, which review all available genetic or physiological information to subsequently identify which genes, proteins, metabolites, or functions change the most between states (but see Reilly et al. 2013; Hudson et al. 2024). Many articles employed biological assays to measure enzyme activity or content, as an approximation of the metabolic scope of a tissue, as metabolic depression can be observed by reduced enzyme levels or function (Flanigan et al. 1990).

Our untargeted approach led to the identification of TRAPP, SNARE, and Arp2/3 complexes, which is novel and highlights the possible importance of membrane remodeling and/or membrane metabolism in the aestivation phenotype. The identification of many genes involved in angiotensin regulation is also novel, although studies of hibernation and hypoxia in other organisms have pointed to its possible involvement (Khudyakov et al. 2021; Bai et al. 2019; Talaei et al. 2012). The role of cell-cycle progression is also of interest and has not been expansively investigated previously, although it was indicated as important in *C. alboguttata* (Reilly et al. 2013). Both cell proliferation and angiogenesis are in part regulated by the NFKB1 transcription factor, which has been shown to be involved in the aestivation response in amphibians (Maistrovski 2011). Similarly, the two other untargeted studies on aestivation in amphibians that we are aware of (Reilly et al. 2013; Hudson et al. 2024), also provided insight into novel mechanisms, such as the involvement of antiapoptotic mechanisms and the possibility that tissues retain pools of mRNA and glycolysis intermediates poised for rapid translation and catabolism when the animal awakes.

Conclusion

There has been great scientific curiosity as well as medical interest in understanding how animals survive and recover from periods of dormancy while maintaining functional organ systems. For example, induced suspended animation is a hypometabolic state of medical interest because it can preserve organ function during life-threatening conditions (Hartmann et al. 2017). Nonetheless, this procedure causes other physiological problems. However, if some of the physiological processes that aestivators or hibernators perform in order to survive a hypometabolic state could be induced in human medicine, the procedure could be improved

(Hartmann et al. 2017). In our review of the literature outside of amphibians, many genes that we highlight have been investigated in terms of cancer tumor states of dormancy versus proliferation (Ho et al. 2020), atrial fibrosis (Yoshikawa et al. 2012), and organ atrophy (Chazarin et al. 2019b). However, most studies of any type of dormancy have been focused on hibernation in mammals. Here we identified some processes overlapping with prior targeted studies on energy shifts in amphibians and other species, but we also highlight possible new processes such as protein and membrane trafficking (TRAPP, SNARE, and Arp2/3 complexes). Thus, studying the aestivation phenotype in amphibians presents novel insight into processes that permit such a fascinating adaptation, which could hold promise for human medicine.

Data and code accessibility statement

All data and code are available as supplementary materials

Supplementary Material

Appendix A1. Script for gene trees based on NCBI gene annotations.

Appendix A2. R script for RER convergence analyses.

Appendix A3. R script for gene ontology analyses.

Appendix A4. Additional results and figures.

Appendix A5. List of clusters and associated annotation files from the Search Tool for the Retrieval of Interacting Genes/Proteins database STRING (Szklarczyk et al., 2023).

Table S1. List of genes, metabolites, miRNAs, or proteins analyzed during aestivation or water restriction found in the literature review (see Methods section).

Table S2. List of genes and proteins used for the comparison between literature and RER results.

Table S3. Full results of the RER analyses.

Table S4. List of genes and terms that were significantly enriched in the GO analyses based on the RER significant gene set compared to the background gene set.

Literature Cited

Akat, E., H. Arıkan, and B. Göçmen. 2014. Histochemical and biometric study of the gastrointestinal system of *Hyla orientalis* (Bedriaga, 1890) (Anura, Hylidae). Eur J Histochem 58:291–295. DOI: https://doi.org/10.4081/ejh.2014.2452

Alexa, A., and J. Rahnenführer. 2024. Gene set enrichment analysis with topGO. DOI: https://doi.org/10.18129/B9.bioc.topGO

Amey, A.P., and G.C. Grigg. 1995. Lipid-reduced evaporative water loss in two arboreal hylid frogs. Comp. Biochem. Physiol. I I I A:283–291.

AmphibiaWeb. 2024. AmphibiaWeb. University of California, Berkeley, CA, USA. Available at https://amphibiaweb.org.

Bai, L., B. Liu, C. Ji, S. Zhao, S. Liu, Rong Wang, W. Wang et al. 2019. Hypoxic and cold adaptation insights from the himalayan marmot genome. iScience 11:519–530. DOI: https://doi.org/10.1016/j.isci.2018.11.034

Bateman, A., M.J. Martin, S. Orchard, M. Michele, A. Adesina, S. Ahmad, E.H. Bowler-Barnett et al. 2025. UniProt: the Universal Protein Knowledgebase in 2025. Nucleic Acids Res 53:D609–D617. DOI: https://doi.org/10.1093/nar/gkae1010

Bauerschmitt, H., S. Funes, and J.M. Herrmann. 2008. The membrane-bound GTPase Guf1 promotes mitochondrial protein synthesis under suboptimal conditions. J Biol Chem 283:17139–17146. DOI: https://doi.org/10.1074/jbc.M710037200

Bayomy, M.F.F., A.G. Shalan, S.D. Bradshaw, P.C. Withers, T. Stewart, and G. Thompson. 2002. Water content, body weight and acid mucopolysaccharides, hyaluronidase and b-glucuronidase in response to aestivation in Australian desert frogs. Comp Biochem Physiol Part A 131:881–892.

Berman, D.I., N.A. Bulakhova, and E.N. Meshcheryakova. 2019. The Siberian wood frog survives for months underwater without oxygen. Sci Rep 9. DOI: https://doi.org/10.1038/s41598-018-31974-6

Biggar, K.K., C.W. Wu, S.N. Tessier, J. Zhang, F. Pifferi, M. Perret, and K.B. Storey. 2015. Modulation of gene expression in key survival pathways during daily torpor in the gray mouse lemur, *Microcebus murinus*. Genom Proteom Bioinform13:111–118. DOI: https://doi.org/10.1016/j.gpb.2015.03.001

Biggar, Y., W.A. Ingelson-Filpula, and K.B. Storey. 2022. Pro- and anti-apoptotic microRNAs are differentially regulated during estivation in *Xenopus laevis*. Gene 819. DOI: https://doi.org/10.1016/j.gene.2022.146236

Booth, D.T. 2006. Effect of soil type on burrowing behavior and cocoon formation in the green-striped burrowing frog, *Cyclorana alboguttata*. Can J Zool 84:832–838. DOI: https://doi.org/10.1139/Z06-062

Borah, B.K., Z. Renthlei, and A.K. Trivedi. 2020. Hypothalamus but not liver retains daily expression of clock genes during hibernation in terai tree frog (*Polypedates teraiensis*). Chronobiol Int 37:485–492. DOI: https://doi.org/10.1080/07420528.2020.1726373

Capraro, A., D. O'Meally, S.A. Waters, H.R. Patel, A. Georges, and P.D. Waters. 2019. Waking the sleeping dragon: Gene expression profiling reveals adaptive strategies of the hibernating reptile *Pogona vitticeps*. BMC Genomics 20. DOI: https://doi.org/10.1186/s12864-019-5750-x

Cartledge, V.A., P.C. Withers, K.A. McMaster, G.G. Thompson, and S.D. Bradshaw. 2006. Water balance of field-excavated aestivating Australian desert frogs, the cocoon-forming

Neobatrachus aquilonius and the non-cocooning *Notaden nichollsi* (Amphibia: Myobatrachidae). J Exp Biol 209:3309–3321. DOI: https://doi.org/10.1242/jeb.02393

Chauvet, J., Y. Ouedraogo, G. Michel, and R. Acher. 1993. Vasotocin and hydrin 2 (vasotocinyl-gly) in the African toad *Bufo regularis*: Study under various environmental conditions. Comp Biochem Physiol 104:497–502.

Chazarin, B., K.B. Storey, A. Ziemianin, S. Chanon, M. Plumel, I. Chery, C. Durand et al. 2019a. Metabolic reprogramming involving glycolysis in the hibernating brown bear skeletal muscle. Front Zool 16. DOI: https://doi.org/10.1186/s12983-019-0312-2

Chazarin, B., A. Ziemianin, A.L. Evans, E. Meugnier, E. Loizon, J.M. Arnemo, J.E. Swenson et al. 2019b. Limited oxidative stress favors resistance to skeletal muscle atrophy in hibernating brown bears (*Ursus Arctos*). Antioxidants 8. DOI: https://doi.org/10.3390/antiox8090334

Cheng, S., and M. Schuh. 2024. Two mechanisms repress cyclin B1 translation to maintain prophase arrest in mouse oocytes. Nat Comm15. DOI: https://doi.org/10.1038/s41467-024-54161-w

Chikina, M., N. Clark, A. Kowalczyk, W. Mao, W. Meyer, and R. Partha. 2025. RERconverge: Analysis of convergence between organismal traits and DNA/Protein Sequences.Rpackage. DOI: https://doi.org/10.18129/B9.bioc.topGO

Chikina, M., J.D. Robinson, and N.L. Clark. 2016. Hundreds of genes experienced convergent shifts in selective pressure in marine mammals. Mol Biol Evol 33:2182–2192. DOI: https://doi.org/10.1093/molbev/msw112

Compton, Z.T., W. Mellon, V.K. Harris, S. Rupp, D. Mallo, S.E. Kapsetaki, M. Wilmot et al. 2025. Cancer Prevalence across Vertebrates. Cancer Discov 15:227–244. DOI: https://doi.org/10.1158/2159-8290.CD-24-0573

Cowan, K.J., J.A. Macdonald, J.M. Storey, K., and B. Storey. 2000. Metabolic reorganization and signal transduction during estivation in the spadefoot toad. Exp Biol Online 5:61–85.

Cowan, K.J., and K.B. Storey. 2002. Urea and KCI have differential effects on enzyme activities in liver and muscle of estivating versus nonestivating species. Biochem Cell Biol 80:745–755. DOI: https://doi.org/10.1139/o02-144

Cramp, R.L., C.E. Franklin, and E.A. Meyer. 2005. The impact of prolonged fasting during aestivation on the structure of the small intestine in the green-striped burrowing frog, *Cyclorana alboguttata*. Acta Zool 86:13–24. DOI: https://doi.org/10.1111/j.0001-7272.2005.00180.x

Cramp, R.L., S.M. Kayes, E.A. Meyer, and C.E. Franklin. 2009. Ups and downs of intestinal function with prolonged fasting during aestivation in the burrowing frog, *Cyclorana alboguttata*. J Exp Biol 212:3656–3663. DOI: https://doi.org/10.1242/jeb.027748

Cullen, P.J. 2008. Endosomal sorting and signaling: an emerging role for sorting nexins. Nat Rev Mol Cell Biol 9:574–582.

Cutrell, S., I.S. Alhomoud, A. Mehta, A.H. Talasaz, B. Van Tassell, and D.L. Dixon. 2023. ACE-Inhibitors in hypertension: A historical perspective and current insights. Curr Hypertens Rep 25:243–250. DOI: https://doi.org/10.1007/s11906-023-01248-2

Dang, K., H.J. Yu, S.H. Xu, T.R. Ma, H.P. Wang, Y. Li, Z. Li, and Y.F. Gao. 2020. Remarkable homeostasis of protein sialylation in skeletal muscles of hibernating daurian ground

squirrels (*Spermophilus dauricus*). Front Physiol 11. DOI: https://doi.org/10.3389/fphys.2020.00037

Dawson, N.J., Y. Biggar, A.I. Malik, and K.B. Storey. 2018. Increased transcript levels and kinetic function of pyruvate kinase during severe dehydration in aestivating African clawed frogs, *Xenopus laevis*. Comp Biochem Physiol B Biochem Mol Biol 224:245–252. DOI: https://doi.org/10.1016/j.cbpb.2018.01.003

Dyer, S.C., O. Austine-Orimoloye, A.G. Azov, M. Barba, I. Barnes, V.P. Barrera-Enriquez, A. Becker et al. 2025. Ensembl 2025. Nucleic Acids Res 53:D948–D957. DOI: https://doi.org/10.1093/nar/gkae1071

Emms, D.M., and S. Kelly. 2019. OrthoFinder: Phylogenetic orthology inference for comparative genomics. Genome Biol 20. DOI: https://doi.org/10.1186/s13059-019-1832-y

Fan, C., Y. Liu, Y. Wang, A. Zhang, W. Xie, H. Zhang, Q. Weng, and M. Xu. 2022. Expression of glycogenic genes in the oviduct of Chinese brown frog (*Rana dybowskii*) during pre-brumation. Theriogenology 185:78–87. DOI: https://doi.org/10.1016/j.theriogenology.2022.03.006

Fedorov, V.B., A. Garreau, Ø. Tøien, B.M. Barnes, and A. V. Goropashnaya. 2025. Transcriptome remodeling and adaptive preservation of muscle protein content in hibernating black bears. bioRxiv preprint 1–22. DOI: https://doi.org/10.1101/2025.03.06.641932

Flanigan, J., P. Withers, K. Storey, and M. Guppy. 1990. Changes in enzyme binding and activity during aestivation in the frog *Neobatrachus pelobatoides*. Comp Biochem Physiol 96B:67–71.

Flanigan, J.E., and M. Guppy. 1997. Metabolic depression and sodium-potassium ATPase in the aestivating frog, *Neobatrachus kunapalari*. J Comp Physiol B 167:135–47.

Fuery, C.J., P.C. Withers, A.A. Hobbs, and M. Guppy. 1998. The role of protein synthesis during metabolic depression in the Australian desert frog *Neobatrachus centralis*. Comp Biochem Physiol 119:469–476.

Giraud-Billoud, M., D.C. Moreira, M. Minari, A. Andreyeva, E.G. Campos, J.M. Carvajalino-Fernández et al. 2024. REVIEW: Evidence supporting the 'preparation for oxidative stress' (POS) strategy in animals in their natural environment. Comp Biochem Physiol A Mol Integr Physiol 293. DOI: https://doi.org/10.1016/j.cbpa.2024.111626

González Nicolini, M. V, A.A. Orezzoli, and M.J. Villar. 1998. An inmunohistochemical study of temperature-related changes in galanin and nitric oxide synthase immunoreactivity in the hypothalamus of the toad. Gen Comp Endocrinol 110:175–181.

Hampton, M., R.G. Melvin, and M.T. Andrews. 2013. Transcriptomic analysis of brown adipose tissue across the physiological extremes of natural hibernation. PLoS One 8. DOI: https://doi.org/10.1371/journal.pone.0085157

Hartmann, C., B. Nussbaum, E. Calzia, P. Radermacher, and M. Wepler. 2017. Gaseous mediators and mitochondrial function: The future of pharmacologically induced suspended animation? Front Physiol 8. DOI: https://doi.org/10.3389/fphys.2017.00691

Hawkins, L.J., and K.B. Storey. 2020. Advances and applications of environmental stress adaptation research. Comp Biochem Physiol A Mol Integr Physiol 240:e110623. DOI: https://doi.org/10.1016/j.cbpa.2019.110623

Hermes-Lima, M., D.C. Moreira, G.A. Rivera-Ingraham, M. Giraud-Billoud, T.C. Genaro-Mattos, and É.G. Campos. 2015. Preparation for oxidative stress under hypoxia and

metabolic depression: Revisiting the proposal two decades later. Free Radic Biol Med 89:1122–1143. DOI: https://doi.org/10.1016/j.freeradbiomed.2015.07.156

Ho, K.H., P.H. Chen, C.M. Chou, C.M. Shih, Y.T. Lee, C.H. Cheng, and K.C. Chen. 2020. A Key Role of DNA Damage-Inducible Transcript 4 (DDIT4) Connects autophagy and GLUT3-mediated stemness to desensitize temozolomide efficacy in glioblastomas. Neurotherapeutics 17:1212–1227. DOI: https://doi.org/10.1007/s13311-019-00826-0

Hou, D.M., T. Jia, H.J. Wang, Z.K. Wang, and W.L. Zhu. 2023. Differentially expressed genes analysis of brown adipose tissue during cold acclimation in male tree shrews (*Tupaia belangeri*) based on RNA-Seq. Pak J Zool 55:591–600. DOI: https://doi.org/10.17582/journal.pjz/20211210131248

Huang, W., C.C. Liao, Y. Han, J Lv, M. Lei, Y. Li, Q. Lv, et al. 2020. Co-activation of Akt, Nrf2, and NF-κB signals under UPRER in torpid *Myotis ricketti* bats for survival. Commun Biol 3. DOI: https://doi.org/10.1038/s42003-020-01378-2

Hudson, N.J., R.L. Cramp, and C.E. Franklin. 2024. Dramatic genome-wide reprogramming of mRNA in hypometabolic muscle. Comp Biochem Physiol B Biochem Mol Biol 272. DOI: https://doi.org/10.1016/j.cbpb.2024.110952

Hughes, M.K., and A.L. Hughes. 1993. Evolution of duplicate genes in a tetraploid animal, *Xenopus laevis*. Mol Biol Evol 10:1360.

IUCN. 2024. The IUCN Red List of Threatened Species. Version 2023-1. http://www.iucnredlist.org. Downloaded October 11, 2024.

Jansen, H.T., S. Trojahn, M.W. Saxton, C.R. Quackenbush, B.D. Evans Hutzenbiler, O.L. Nelson, O.E. Cornejo, C.T. Robbins, and J.L. Kelley. 2019. Hibernation induces widespread

transcriptional remodeling in metabolic tissues of the grizzly bear. Commun Biol 2. DOI: https://doi.org/10.1038/s42003-019-0574-4

Jiang, C., K.B. Storey, H. Yang, and L. Sun. 2023. Aestivation in Nature: Physiological strategies and evolutionary adaptations in hypometabolic states. Int J Mol Sci 24:e14093. DOI: https://doi.org/10.3390/ijms241814093

Jones, R.M. 1980. Metabolic consequences of accelerated urea synthesis during seasonal dormancy of spadefoot toads, *Scaphiopus couchi* and *Scaphiopus multip*licatus. J Exp Zool 212:255–267. DOI: https://doi.org/10.1002/jez.1402120212

Jopling, C., G. Suñé, A. Faucherre, C. Fabregat, J. Carlos, and I. Belmonte. 2012. Molecular cardiology hypoxia induces myocardial regeneration in zebrafish. Circulation 126:3017–3027. DOI: https://doi.org/10.1161/CIRCULATIONAHA

Jørgensen, C.B. 1997. Urea and amphibian water economy. Comp Biochem Physiol 117:161–170.

Katoh, K., and D.M. Standley. 2013. MAFFT multiple sequence alignment software version 7: Improvements in performance and usability. Mol Biol Evol 30:772–780. DOI: https://doi.org/10.1093/molbev/mst010

Katzenback, B.A., N.J. Dawson, and K.B. Storey. 2014. Purification and characterization of a urea sensitive lactate dehydrogenase from the liver of the African clawed frog, X*enopus laevis*. J Comp Physiol B 184:601–611. DOI: https://doi.org/10.1007/s00360-014-0824-1

Kay, R.R. 2021. Macropinocytosis: Biology and mechanisms. Cells Dev 168. DOI: https://doi.org/10.1016/j.cdev.2021.203713

Khosravi, S., and M.E. Harner. 2020. The MICOS complex, a structural element of mitochondria with versatile functions. Biol Chem 401:765–778. DOI: https://doi.org/10.1515/hsz-2020-0103

Khudyakov, J.I., M.D. Treat, M.C. Shanafelt, J.S. Deyarmin, B.A. Neely, and F. van Breukelen. 2021. Liver proteome response to torpor in a basoendothermic mammal, *Tenrec ecaudatus*, provides insights into the evolution of homeothermy. Am J Physiol Regul Integr Comp Physiol 321:R614–R624. DOI: https://doi.org/10.1152/ajpregu.00150.2021

Kowalczyk, A., W.K. Meyer, R. Partha, W. Mao, N.L. Clark, and M. Chikina. 2019. RERconverge: An R package for associating evolutionary rates with convergent traits. Bioinformatics 35:4815–4817. DOI: https://doi.org/10.1093/bioinformatics/btz468

Kumar, S., M. Suleski, J.M. Craig, A.E. Kasprowicz, M. Sanderford, M. Li, G. Stecher, and S.B. Hedges. 2022. TimeTree 5: An expanded resource for species divergence times. Mol Biol Evol 39. DOI: https://doi.org/10.1093/molbev/msac174

Lang, M.J., J.Y. Martinez-Marquez, D.C. Prosser, L.R. Ganser, D. Buelto, B. Wendland, and M.C. Duncan. 2014. Glucose starvation inhibits autophagy via vacuolar hydrolysis and induces plasma membrane internalization by down-regulating recycling. J Biol Chem 289:16736–16747. DOI: https://doi.org/10.1074/jbc.M113.525782

Lauc, G., and M. Wuhrer. 2017. High throughput glycomics and glycoproteomics. Methods and protocols. Humana Press, New York, NY.

Liedtke, H.C., F. Cruz, J. Gómez-Garrido, D. Fuentes Palacios, M. Marcet-Houben, M. Gut, T. Alioto, T. Gabaldón, and I. Gomez-Mestre. 2022. Chromosome-level assembly, annotation and phylome of *Pelobates cultripes*, the western spadefoot toad. DNA Research 29. DOI: https://doi.org/10.1093/dnares/dsac013

Luu, B.E., L.J. Hawkins, and K.B. Storey. 2021. Insights from a vertebrate model organism on the molecular mechanisms of whole-body dehydration tolerance. Mol Cell Biochem 476:2381–2392. DOI: https://doi.org/10.1007/s11010-021-04072-x

Luu, B.E., and K.B. Storey. 2015. Dehydration triggers differential microRNA expression in *Xenopus laevis* brain. Gene 573:64–69. DOI: https://doi.org/10.1016/j.gene.2015.07.027

Luu, B.E., S. Wijenayake, A.I. Malik, and K.B. Storey. 2018. The regulation of heat shock proteins in response to dehydration in *Xenopus laevis*. Cell Stress Chaperones 23:45–53. DOI: https://doi.org/10.1007/s12192-017-0822-9

Luu, B.E., Y. Zhang, and K.B. Storey. 2020. The regulation of Akt and FoxO transcription factors during dehydration in the African clawed frog (*Xenopus laevis*). Cell Stress Chaperones 25:887–897. DOI: https://doi.org/10.1007/s12192-020-01123-y/Published

Ma, Y., Y. Chen, Y. Li, S. Chen, C. Zhu, Q. Liu, L. Li, et al. 2024. Seasonal modulation of the testis transcriptome reveals insights into hibernation and reproductive adaptation in *Onychostoma macrolepis*. Fish Physiol Biochem 50:2083–2097. DOI: https://doi.org/10.1007/s10695-024-01335-4

Madelaire, C.B., F.R. Gomes, and I. Sokolova. 2020. Biomarker-based assessment of the muscle maintenance and energy status of anurans from an extremely seasonal semi-arid environment, the Brazilian Caatinga. Comp Biochem Physiol A Mol Integr Physiol 240. DOI: https://doi.org/10.1016/j.cbpa.2019.110590

Maistrovski, Y. 2011. Regulation of anti-apoptotic pathways in skeletal muscle and liver of an estivating species, *Xenopus laevis*. Carleton University, Ottawa, Ontario, Canada.

Malik, A.I., J.M. Storey, and K.B. Storey. 2023. Regulation of the unfolded protein response during dehydration stress in African clawed frogs, *Xenopus laevis*. Cell Stress Chaperones 28:529–540. DOI: https://doi.org/10.1007/s12192-022-01275-z

Malik, A.I., and K.B. Storey. 2011. Transcriptional regulation of antioxidant enzymes by FoxO1 under dehydration stress. Gene 485:114–119. DOI: https://doi.org/10.1016/j.gene.2011.06.014

Malik, A.L., and K.B. Storey. 2009. Activation of extracellular signal-regulated kinases during dehydration in the African clawed frog, *Xenopus laevis*. J Exp Biol 212:2595–2603. DOI: https://doi.org/10.1242/jeb.030627

Manor, J., D. Calame, C. Gijavanekar, K. Fisher, J. Hunter, E. Mizerik, C. Bacino, F. Scaglia, and S.H. Elsea. 2022. NAXE deficiency: A neurometabolic disorder of NAD(P)HX repair amenable for metabolic correction. Mol Genet Metab 136:101–110. DOI: https://doi.org/10.1016/j.ymgme.2022.04.003

Mayhew, W.W. 1968. Biology of desert amphibians and reptiles. Pp. 195–356 in Desert Biology; special topic on the physical and biological aspects of arid regions (G. Brown, ed.). Academic Press, New York, NY.

McClanahan, L. 1972. Changes in body fluids of burrowed Spadefoot toads as a function of soil water potential. Copeia 1972:209–216.

Meyer, W. 2024. RERconverge Analysis Walkthrough. 1–29 pp.

Minh, B.Q., H.A. Schmidt, O. Chernomor, D. Schrempf, M.D. Woodhams, A. Von Haeseler, R. Lanfear, and E. Teeling. 2020. IQ-TREE 2: New models and efficient methods for phylogenetic inference in the genomic era. Mol Biol Evol 37:1530–1534. DOI: https://doi.org/10.1093/molbev/msaa015

Naguib, A., T. Sandmann, F. Yi, R.J. Watts, J.W. Lewcock, and W.E. Dowdle. 2019. SUPT4H1 depletion leads to a global reduction in RNA. Cell Rep 26:45-53.e4. DOI: https://doi.org/10.1016/j.celrep.2018.12.004

Naranjo, M., S.A. Breedon, and K.B. Storey. 2023. Cardiac microRNA expression profile in response to estivation. Biochimie 210:22–34. DOI: https://doi.org/10.1016/j.biochi.2023.01.001

Navas, C.A., and J.E. Carvalho. 2010. Aestivation molecular and physiological aspects. (C.A. Navas and J.E. Carvalho, eds.). Springer-Verlag, Berlin Heidelberg, Germany.

Ochoa-Ochoa, L.M., J.D. Vásquez-Restrepo, M. Masache, and R.D. Tarvin. 2025. Slowing down: A macroevolutionary approach to the hypometabolic strategies of amphibians. bioRxiv preprint DOI: https://doi.org/10.1101/2025.07.19.665691

O'Leary, N.A., E. Cox, J.B. Holmes, W. R. Anderson, R. Falk, V. Hem, M.T.N. Tsuchiya et al. 2024. Exploring and retrieving sequence and metadata for species across the tree of life with NCBI Datasets. Sci Data 11. DOI: https://doi.org/10.1038/s41597-024-03571-y

Pakay, J.L., A.A. Hobbs, S.R. Kimball, and M. Guppy. 2003. The role of eukaryotic initiation factor 2α during the metabolic depression associated with estivation. J Exp Biol 206:2363–2371. DOI: https://doi.org/10.1242/jeb.00422

Paradis, E., and K. Schliep. 2019. Ape 5.0: An environment for modern phylogenetics and evolutionary analyses in R. Bioinformatics 35:526–528. DOI: https://doi.org/10.1093/bioinformatics/bty633

Patnaik, P., and D. Das Sahoo. 2021. Variations in oxidative stress and antioxidant defense level during different phases of hibernation in common Asian toad, *Duttaphrynus melanostictus*. Biol Open 10. DOI: https://doi.org/10.1242/bio.058567

Pinder, A.W., K.B. Storey, and G.R. Ultsch. 1992. Estivation and Hibernation. Pp. 250–274 in Environmental Physiology of the Amphibians (M.E. Feder and W.W. Burggren, eds.). The University of Chicago Press, Chicago.

Portik, D.M., J.W. Streicher, and J.J. Wiens. 2023. Frog phylogeny: A time-calibrated, species-level tree based on hundreds of loci and 5,242 species. Mol Phylogenet Evol 188. DOI: https://doi.org/10.1016/j.ympev.2023.107907

Pourazami, S. 2024. Snails in a dry sauna: A transcriptomic tale of *Bostryx conspersus*. Norwegian University of Science and Technology - NTNU, Trondheim, Norway.

R Core Team. 2024. R: A Language and Environment for Statistical Computing.

Reilly, B.D., D.I. Schlipalius, R.L. Cramp, P.R. Ebert, and C.E. Franklin. 2013. Frogs and estivation: Transcriptional insights into metabolism and cell survival in a natural model of extended muscle disuse. Physiol Genomics 45:377–388. DOI: https://doi.org/10.1152/physiolgenomics.00163.2012

Revell, L.J. 2024. phytools 2.0: an updated R ecosystem for phylogenetic comparative methods (and other things). PeerJ 12:e16505. DOI: https://doi.org/10.7717/peerj.16505

Rotty, J.D., C. Wu, and J.E. Bear. 2013. New insights into the regulation and cellular functions of the ARP2/3 complex. Nat Rev Mol Cell Biol 14:7–12. DOI: https://doi.org/10.1038/nrm3492

Sacher, M., Y.G. Kim, A. Lavie, B.H. Oh, and N. Segev. 2008. The TRAPP complex: Insights into its architecture and function. Traffic 9:2032–2042. DOI: https://doi.org/10.1111/j.1600-0854.2008.00833.x

Sadowski-Fugitt, L.M., C.R. Tracy, K.A. Christian, and J.B. Williams. 2012. Cocoon and epidermis of Australian *Cyclorana* frogs differ in composition of lipid classes that affect

Water loss. Physiological and Biochemical Zoology 85:40–50. DOI: https://doi.org/10.1086/663695

Seymour, R.S. 1973. Gas exchange in spadefoot toads beneath the ground. Copeia 1973:452–460.

Shalan, A.G., S.D. Bradshaw, P.C. Withers, G. Thompson, M.F.F. Bayomy, F.J. Bradshaw, and T. Stewart. 2004. Spermatogenesis and plasma testosterone levels in Western Australian burrowing desert frogs, *Cyclorana platycephala*, *Cyclorana maini*, and *Neobatrachus sutor*, during aestivation. Gen Comp Endocrinol 136:90–100. DOI: https://doi.org/10.1016/j.ygcen.2003.12.005

Shannon, P., A. Markiel, O. Ozier, N.S. Baliga, J.T. Wang, D. Ramage, N. Amin, B. Schwikowski, and T. Ideker. 2003. Cytoscape: A software environment for integrated models of biomolecular interaction networks. Genome Res 13:2498–2504. DOI: https://doi.org/10.1101/gr.1239303

Sjodin, B. 2023. Unravelling climate and high elevation adaptation in the American pika (*Ochotona princeps*) through a comparative genomics framework. The University of British Columbia.

Sparks, K. 2021. Gene expression of hypoxia-inducible factor (HIF-1A), its regulators, and its putative downstream targets in ventricle and telencephalon of the anoxia-tolerant turtle (*Trachemys scripta*). University of Alaska Anchorage, Anchorage.

Storey, K.B. 2000. Turning down the fires of life: metabolic regulation of hibernation and estivation. Comp Biochem Physiol B Biochem Mol Biol 126:S90. DOI: https://doi.org/10.1016/s0305-0491(00)80178-9

Storey, K.B. 2002. Life in the slow lane: molecular mechanisms of estivation. 133. 733–754 pp.

Storey, K.B., and J.M. Storey. 2004. Metabolic rate depression in animals: Transcriptional and translational controls. Biol Rev 79:207–233. DOI: https://doi.org/10.1017/S1464793103006195

Storey, K.B., and J.M. Storey. 2007. Tribute to P. L. Lutz: Putting life on “pause” - Molecular regulation of hypometabolism. J Exp Biol 210:1700–1714. DOI: https://doi.org/10.1242/jeb.02716

Storey, K.B., and J.M. Storey. 2010. Metabolic Regulation and Gene Expression During Aestivation. Pp. 25–45 in Aestivation: Molecular and physiological aspects (C.A. Navas and J.E. Carvalho, eds.). Springer-Verlag, Berlin Heidelberg, Germany.

Storey, K.B., and J.M. Storey. 2012. Aestivation: Signaling and hypometabolism. J Exp Biol 215:1425–1433. DOI: https://doi.org/10.1242/jeb.054403

Supek, F., M. Bošnjak, N. Škunca, and T. Šmuc. 2011. Revigo summarizes and visualizes long lists of gene ontology terms. PLoS One 6. DOI: https://doi.org/10.1371/journal.pone.0021800

Szklarczyk, D., R. Kirsch, M. Koutrouli, K. Nastou, F. Mehryary, R. Hachilif, A.L. Gable et al.2023. The STRING database in 2023: protein-protein association networks and functional enrichment analyses for any sequenced genome of interest. Nucleic Acids Res 51:D638–D646. DOI: https://doi.org/10.1093/nar/gkac1000

Taiwo, O.O., S.A. Breedon, and K.B. Storey. 2024. Epigenetic Regulation by Histone Methylation and Demethylation in Freeze-Tolerant Frog Kidney. Cell Biochem Funct 42. DOI: https://doi.org/10.1002/cbf.70036

Talaei, F., H.R. Bouma, M.N. Hylkema, A.M. Strijkstra, A.S. Boerema, M. Schmidt, and R.H. Henning. 2012. The role of endogenous H2S formation in reversible remodeling of lung

tissue during hibernation in the Syrian hamster. J Exp Biol 215:2912–2919. DOI: https://doi.org/10.1242/jeb.067363

Tingaud-Sequeira, A., J.J. Lozano, C. Zapater, D. Otero, M. Kube, R. Reinhardt, and J. Cerdà. 2013. A rapid transcriptome response is associated with desiccation resistance in aerially-exposed killifish embryos. PLoS One 8. DOI: https://doi.org/10.1371/journal.pone.0064410

Torres-Dimas, E., A. Cruz-Ramírez, and R.M. Bermúdez-Cruz. 2022. Cancer in Amphibia, a rare phenomenon? Cell Biol Int 46:1992–1998. DOI: https://doi.org/10.1002/cbin.11888

Ungar, D., and F.M. Hughson. 2003. SNARE protein structure and function. Annu Rev Cell Dev Biol 19:493–517.

Uno, Y. 2021. Inference of evolution of vertebrate genomes and chromosomes from genomic and cytogenetic analyses using amphibians. 24:3–12.

Vieira de Andrade, D., C.R. Bevier, and J. Eduardo de Carvalho. 2016. Amphibian and reptile adaptations to the environment. Interplay between physiology and behavior. Taylor & Francis Group, Boca Raton, FL.

Voet, D., J.G. Voet, and C.W. Pratt. 2008. Fundamentals of biochemistry: Life at the molecular level. 3rd Edition. John Wiley & Sons, Inc., Hoboken, NJ.

Wang, C., Z. Guo, C. Chu, Y. Lu, X. Zhang, and X. Zhan. 2023. Two assembly modes for SIN3 histone deacetylase complexes. Cell Discov 9. DOI: https://doi.org/10.1038/s41421-023-00539-x

Waskova-Arnostova, P., B. Elsnicova, D. Kasparova, D. Hornikova, F. Kolar, J. Novotny, J. Zurmanova, and Z.J. Cardioprotective. 2015. Cardioprotective adaptation of rats to intermittent hypobaric hypoxia is accompanied by the increased association of hexokinase

with mitochondria. J Appl Physiol 119:1487–1493. DOI: https://doi.org/10.1152/japplphysiol.01035.2014.-Chronic

Wilsterman, K., M.A. Ballinger, and C.M. Williams. 2021. A unifying, eco-physiological framework for animal dormancy. Funct Ecol 35:11–31. DOI: https://doi.org/10.1111/1365-2435.13718

Wu, C.W., K.K. Biggar, and K.B. Storey. 2013. Dehydration mediated microRNA response in the African clawed frog *Xenopus laevis*. Gene 529:269–275. DOI: https://doi.org/10.1016/j.gene.2013.07.064

Wu, C.W., S.N. Tessier, and K.B. Storey. 2017. Regulation of the insulin-Akt signaling pathway and glycolysis during dehydration stress in the African clawed frog *Xenopus laevis*. Biochemistry and Cell Biology 95:663–671. DOI: https://doi.org/10.1139/bcb-2017-0117

Wu, C.W., S.N. Tessier, and K.B. Storey. 2020. Dehydration stress alters the mitogen-activated-protein kinase signaling and chaperone stress response in *Xenopus laevis*. Comp Biochem Physiol B Biochem Mol Biol 246–247. DOI: https://doi.org/10.1016/j.cbpb.2020.110461

Xiao, Y., Y. Wu, K. Sun, Hui Wang1,2, Bing Zhang, S. Song, Z. Du et al. 2015. Differential expression of hepatic genes of the greater horseshoe bat (*Rhinolophus ferrumequinum*) between the summer active and winter torpid states. PLoS One 10. DOI: https://doi.org/10.1371/journal.pone.0145702

Yang, J., W.R. Li, F.H. Lv, S.G. He, S.L.Tian, W.F. Peng, Y.W. Sun et al. 2016. Whole-genome sequencing of native sheep provides insights into rapid adaptations to extreme environments. Mol Biol Evol 33:2576–2592. DOI: https://doi.org/10.1093/molbev/msw129

Yang, Q., X. Zhang, Z. Lu, R. Huang, N.T. Tran, J. Wu, F. Yang et al. 2021. Transcriptome and Metabolome Analyses of Sea Cucumbers *Apostichopus japonicus* in Southern China During the Summer Aestivation Period. Journal of Ocean University of China 20:198–212. DOI: https://doi.org/10.1007/s11802-021-4482-0

Yoshikawa, N., N. Shimizu, T. Maruyama, M. Sano, T. Matsuhashi, K. Fukuda, M. Kataoka et al. 2012. Cardiomyocyte-specific overexpression of HEXIM1 prevents right ventricular hypertrophy in hypoxia-induced pulmonary hypertension in mice. PLoS One 7. DOI: https://doi.org/10.1371/journal.pone.0052522

Zhang, Y., B.E. Luu, and K.B. Storey. 2018. FoxO4 activity is regulated by phosphorylation and the cellular environment during dehydration in the African clawed frog, *Xenopus laevis*. Biochim Biophys Acta Gen Subj 1862:1721–1728. DOI: https://doi.org/10.1016/j.bbagen.2018.05.002

Tables

Table 1. List of amphibian species used in the analyses. All species have Gene Protein-coding, most species have chromosome level annotation and all BUSCO annotations correspond with lineage tetrapoda odb10 (NCIBI accessed May 25, 2025).

	Species	Number of Chromosomes	BUSCO Complete	BUSCO Single Copy	Count Gene Total	Count Gene Protein-coding	Aestivation Bir Literature
Gymnophiona							
Dermophiidae	*Geotrypetes seraphini*	19	96.20%	93.88%	24,027	19,223	0
Siphonopidae	*Microcaecilia unicolor*	14	96.78%	91.75%	26,246	20,868	0
Rhinatrematidae	*Rhinatrema bivittatum*	19	96.59%	93.01%	28,114	21,554	0
Caudata							
Ambystomatidae	*Ambystoma mexicanum*	21	95.86%	93.73%	135,668	24,121	0
Salamandridae	*Pleurodeles waltl*	16	95.01%	92.69%	59,059	22,339	1
Anura							
Ascaphidae	*Ascaphus truei*	22			31,412	31,412	0
Bombinatoridae	*Bombina bombina*	12	93.77%	89.06%	31,613	22,468	0

	Species	Number of Chromosomes	BUSCO Complete	BUSCO Single Copy	Count Gene Total	Count Gene Protein-coding	Aestivation Bir Literature
Bufonidae	*Bufo bufo*	11	95.25%	93.18%	32,600	21,517	1
	Bufo gargarizans	11	91.77%	86.76%	27,589	22,033	0
	Bufotes viridis	11			31,608	31,608	1
Craugastoridae	*Pristimantis euphronides*				4,790	4,779	0
Dendrobatidae	*Dendrobates tinctorius*		94.76%	92.58%	55,177	24,289	0
	Phyllobates terribilis		94.76%	92.84%	126,719	25,510	0
	Ranitomeya imitator	10	95.31%	93.05%	44,421	23,747	0
Dicroglossidae	*Nanorana parkeri*		92.99%	91.51%	21,416	18,958	0
Eleutherodactylida e	*Eleutherodactylus coqui*	13	94.63%	92.62%	61,928	21,776	0
Hylidae	*Dendropsophus ebraccatus*	15	95.80%	93.26%	37,424	22,271	0
	Hyla sarda	13	94.56%	92.84%	102,483	22,847	0
Hyperoliidae	*Hyperolius riggenbachi*	12	93.80%	90.98%	68,148	24,147	0
Leptodactylidae	*Engystomops pustulosus*	11	94.61%	92.73%	71,488	21,963	0
Myobatrachidae	*Pseudophryne corroboree*	12	95.33%	93.60%	186,827	24,591	0
Pipidae	*Hymenochirus boettgeri*	9			20,654	20,654	0

	Species	Number of Chromosomes	BUSCO Complete	BUSCO Single Copy	Count Gene Total	Count Gene Protein-coding	Aestivation Bir Literature
	Xenopus laevis	18	97.49%	45.46%	44,456	34,476	1
	Xenopus tropicalis	10	96.57%	95.03%	28,858	21,826	1
Pelobatidae	*Pelobates cultripes*	14			231,783	32,684	1
	Pelobates fuscus	13	96.55%	94.39%	49,915	20,977	1
Ranidae	*Pyxicephalus adspersus*	14	91.49%	89.96%	24,071	19,416	1
	Rana catesbeiana	13	94.54%	92.03%	47,255	24,438	1
	Rana temporaria	13	95.24%	92.84%	38,300	23,707	0
	Staurois parvus				78,191	78,191	0
Scaphiopodidae	*Spea bombifrons*	13	96.25%	94.92%	42,958	19,086	1

Table 2. The top 10 genes identified by RER as under relatively accelerated evolutionary rates ($p \leq 0.05$). Note: none of these genes were significant after multiple testing corrections. Protein names and functions were copied from the UniProt database on 6/9/25 for entries of *Xenopus laevis* or *Xenopus tropicalis* unless otherwise noted (Dyer et al. 2025). *Denotes genes that were

also associated with significantly enriched GO terms. ^Denotes genes that were present in a STRING gene cluster.

Gene and Protein Names	Protein Function	*Rho*	*N*	p-value
GPRC5B G-protein coupled receptor family C group 5 member B	G-protein coupled receptor involved in the regulation of cell volume (annotation from *Homo sapiens*).	0.617	32	0.00017
TRAPPC6B*^ Trafficking protein particle complex subunit 6B	Component of a transport protein particle complex that may function in specific stages of inter-organelle traffic. Specifically involved in the early development of neural circuitry, likely by controlling the frequency and amplitude of intracellular calcium transients implicated in the regulation of neuron differentiation and survival. (annotation from *Homo sapiens*)	0.564	32	0.00076
FLNB* Filamin B	Connects cell membrane constituents to the actin cytoskeleton. May promote orthogonal branching of actin filaments and links actin filaments to membrane glycoproteins. Anchors various transmembrane proteins to the actin cytoskeleton. Interaction with FLNA may allow neuroblast migration from the ventricular zone into the cortical plate. Various interactions and localizations of isoforms affect myotube morphology and myogenesis. (annotation from *Homo sapiens*)	0.478	45	0.00090
PARVA* Parvin alpha	Plays a role in sarcomere organization and in smooth muscle cell contraction. Required for normal development of the embryonic cardiovascular system, and for normal septation of the heart outflow tract. Plays a role in sprouting angiogenesis and is required for normal adhesion of vascular smooth muscle cells to endothelial cells during blood vessel development. Plays a role in the reorganization of the actin cytoskeleton, formation of lamellipodia and ciliogenesis. Plays a role in the establishment of cell polarity, cell adhesion, cell spreading, and directed cell migration. Within the IPP (ILK-PINCH-PARVIN) complex, binds to F-actin, promoting F-actin bundling, a process required to generate force for actin cytoskeleton reorganization and subsequent dynamic cell adhesion events such as cell spreading and migration (annotation from *Homo sapiens*).	0.553	32	0.00102
TEX264 Testis-expressed protein 264 homolog	Major reticulophagy (also called ER-phagy) receptor that acts independently of other candidate reticulophagy receptors to remodel subdomains of the endoplasmic reticulum into autophagosomes upon nutrient stress, which then fuse with lysosomes for endoplasmic reticulum turnover (annotation from *Homo sapiens*).	0.476	40	0.00189
VPS18* Vacuolar protein sorting-associated protein 18 homolog	Plays a role in vesicle-mediated protein trafficking to lysosomal compartments including the endocytic membrane transport and autophagic pathways. Required for fusion of endosomes and autophagosomes with lysosomes. (annotation from *Homo sapiens*)	0.460	43	0.00190

Gene and Protein Names	Protein Function	*Rho*	*N*	p-value
BRD9* Bromodomain-containing protein 9	Plays a role in chromatin remodeling and regulation of transcription. Acts as a chromatin reader that recognizes and binds acylated histones: binds histones that are acetylated and/or butyrylated.	0.463	42	0.00203
DAD1*^ Dolichyl-diphosphooligosaccharide--protein glycosyltransferase subunit dad1	Subunit of the oligosaccharyl transferase complex that catalyzes the initial transfer of a defined glycan (Glc3Man9GlcNAc2 in eukaryotes) from the lipid carrier dolichol-pyrophosphate to an asparagine residue within an Asn-X-Ser/Thr consensus motif in nascent polypeptide chains, the first step in protein N-glycosylation. N-glycosylation occurs cotranslationally and the complex associates with the Sec61 complex at the channel-forming translocon complex that mediates protein translocation across the endoplasmic reticulum.	0.578	25	0.00247
SCT Secretin	Hormone involved in different processes, such as regulation of the pH of the duodenal content, food intake and water homeostasis. Acts as a key gastrointestinal hormone by regulating the pH of the duodenal content. Secreted by S cells of the duodenum in the crypts of Lieberkuehn and regulates the pH of the duodenum by 1 inhibiting the secretion of gastric acid from the parietal cells of the stomach and 2 stimulating the production of bicarbonate (NaHCO3) from the ductal cells of the pancreas. Production of bicarbonate is essential to neutralize the pH and ensure no damage is done to the small intestine by the gastric acid. Plays a central role in diet induced thermogenesis: acts as a non-sympathetic brown fat activator mediating prandial thermogenesis, which consequently induces satiation. Mechanistically, secretin released by the gut after a meal binds to secretin receptor in brown adipocytes, activating brown fat thermogenesis by stimulating lipolysis, which is sensed in the brain and promotes satiation. Also able to stimulate lipolysis in white adipocytes. Also plays an important role in cellular osmoregulation: released into the systemic circulation in response to hyperosmolality and acts at different levels in the hypothalamus, pituitary and kidney to regulate water homeostasis. Also plays a role in the central nervous system, possibly by acting as a neuropeptide hormone: required for hippocampal synaptic function and neural progenitor cell maintenance. (annotation from *Homo sapiens*)	0.435	45	0.00282
NOS3^ Nitric oxide synthase	Produces nitric oxide (NO) which is a messenger molecule with diverse functions	0.453	40	0.00335

Table 3. The top 10 genes identified by RER as under relatively decelerated evolutionary rates ($p \leq 0.05$). Note: none of these genes were significant in RER after multiple testing corrections. Protein names and functions were copied from the UniProt database on 6/9/25 for entries of *Xenopus laevis* or *Xenopus tropicalis* unless otherwise noted (Dyer et al. 2025). *Denotes genes

that were also associated with significantly enriched GO terms. ^Denotes genes that were present in a STRING gene cluster.

Gene and Protein Names	Protein Function	*Rho*	*N*	p-value
RRM2^ Ribonucleoside-diphosphate reductase subunit M2	S-adenosyl-L-methionine-dependent 2'-O-ribose methyltransferase that catalyzes the formation of 2'-O-methyluridine at position 1369 in the 16S mitochondrial large subunit ribosomal RNA (mtLSU rRNA), a universally conserved modification in the peptidyl transferase domain of the mtLSU rRNA. This activity may require prior 2'-O-methylguanosine modification at position 1370 (Gm1370) by MRM3. Essential for late-stage assembly of mtLSU required for efficient translation of mitochondrial DNA encoded proteins; methyltransferase activity is not required for this function. Essential for mitochondrial respiratory function (annotation from *Homo sapiens*).	-0.614	33	0.00015
UBE2G1^ Ubiquitin-conjugating enzyme E2 G1	Accepts ubiquitin from the E1 complex and catalyzes its covalent attachment to other proteins. In vitro catalyzes 'Lys-48'-, as well as 'Lys-63'-linked polyubiquitination. May be involved in degradation of muscle-specific proteins. (annotation from *Homo sapiens*)	-0.911	10	0.00024
SPACA6^ Sperm acrosome membrane-associated protein 6	Sperm protein required for fusion of sperm with the egg membrane during fertilization. (annotation from *Homo sapiens*)	-0.746	17	0.00059
NDUFB3^ NADH dehydrogenase [ubiquinone] 1 beta subcomplex subunit 3	Accessory subunit of the mitochondrial membrane respiratory chain NADH dehydrogenase (Complex I), that is believed not to be involved in catalysis. Complex I functions in the transfer of electrons from NADH to the respiratory chain. The immediate electron acceptor for the enzyme is believed to be ubiquinone.	-0.509	39	0.00093
RP1 Oxygen-regulated protein 1	Microtubule-associated protein regulating the stability and length of the microtubule-based axoneme of photoreceptors. Required for the differentiation of photoreceptor cells, it plays a role in the organization of the outer segment of rod and cone photoreceptors ensuring the correct orientation and higher-order stacking of outer segment disks along the photoreceptor axoneme. (annotation from *Homo sapiens*)	-0.504	39	0.00108
HEXB Beta-hexosaminidase	Hydrolyzes the non-reducing end N-acetyl-D-hexosamine and/or sulfated N-acetyl-D-hexosamine of glycoconjugates, such as the oligosaccharide moieties from proteins and neutral glycolipids, or from certain mucopolysaccharides. The isozyme B does not hydrolyze each of these substrates, however hydrolyzes efficiently neutral oligosaccharide.	-0.485	41	0.00130
PMF1 Polyamine-modulated factor 1	Part of the MIS12 complex which is required for normal chromosome alignment and segregation and kinetochore formation during mitosis (annotation from *Homo sapiens*)	-0.464	39	0.00295
NPR2*^ Atrial natriuretic peptide receptor 2	Receptor for the C-type natriuretic peptide NPPC/CNP hormone. Has guanylate cyclase activity upon binding of its ligand. May play a role in the regulation of skeletal growth.	-0.435	42	0.00397

Gene and Protein Names	Protein Function	*Rho*	*N*	p-value
MTRF1L*^ Mitochondrial translational release factor 1-like	Mitochondrial peptide chain release factor that directs the termination of translation in response to the peptide chain termination codons UAA and UAG (annotation from *Homo sapiens*)	-0.444	40	0.00409
ATP5F1A*^ ATP synthase F(1) complex subunit alpha, mitochondrial	Subunit alpha, of the mitochondrial membrane ATP synthase complex (F1F0 ATP synthase or Complex V) that produces ATP from ADP in the presence of a proton gradient across the membrane which is generated by electron transport complexes of the respiratory chain.	-0.444	38	0.00528

Table 4. Genes with significant relative evolutionary rates (RERs) that were also the focus of prior studies identified in our literature review.

	Activity	
RER	*Increased*	*Decreased*
Accelerated	DLG1, EIF4ENIF1, GSPT1, and HK1	AUTS2, BFAR, CDKN1B, HHEX, NOS3, SAP30, and YBX1
Decelerated	ANP32B, GPI, JCHAIN, PKM, POLR2B, SARS1, UBE2G1, and UBE2V2	ABRACL, ACE, ADAM23, ANXA4, ATP5PB, DDIT4, GPI, JCHAIN, KIAA1191, MLYCD, MMEL1, NDUFB3, and NDUFS4

Figure legends

Figure 1. Phylogenetic tree of the amphibian species included in the analyses subsetted from Portik et al. (2023) and aggregated *Microcaecilia unicolor* (see methods). Black circles indicate that according to the literature review the species perform aestivation. White circles represent either lack of information or that in the literature has been reported that the species does not aestivate (i.e., *Ascaphus truei*).

Figure 2. Gene network clusters inferred from significantly accelerated RER genes, using *Homo sapiens* for annotation. Grey annotations refer to annotations of similar clusters obtained using *Xenopus tropicalis* annotation information. Nodes with no black outline are interactors inferred by STRING that were not present in our original query set. Permalink to the *H. sapiens* STRING network: https://version-12-0.string-db.org/cgi/network?networkId=boDXLAbScr1l. Permalink to the *X. tropicalis* STRING network: https://version-12-0.string-db.org/cgi/network?networkId=bLnhqSov6Wyj

Figure 3. Gene network clusters inferred from significantly decelerated RER genes, using *Homo sapiens* for annotation. Grey annotations refer to annotations of similar clusters obtained using *Xenopus tropicalis* annotation information. Nodes with no black outline are interactors inferred by STRING that were not present in our original query set. Permalink to the *H. sapiens* STRING network: https://version-12-0.string-db.org/cgi/network?networkId=boDXLAbScr1l. Permalink to the *X. tropicalis* STRING network: https://version-12-0.string-db.org/cgi/network?networkId=b7OklVW1IPb1

Figure 4. Genes related to the central dogma that we identified to have significantly accelerated (+) or decelerated (–) relative evolutionary rates in aestivating amphibians.

Figures

Figure 1

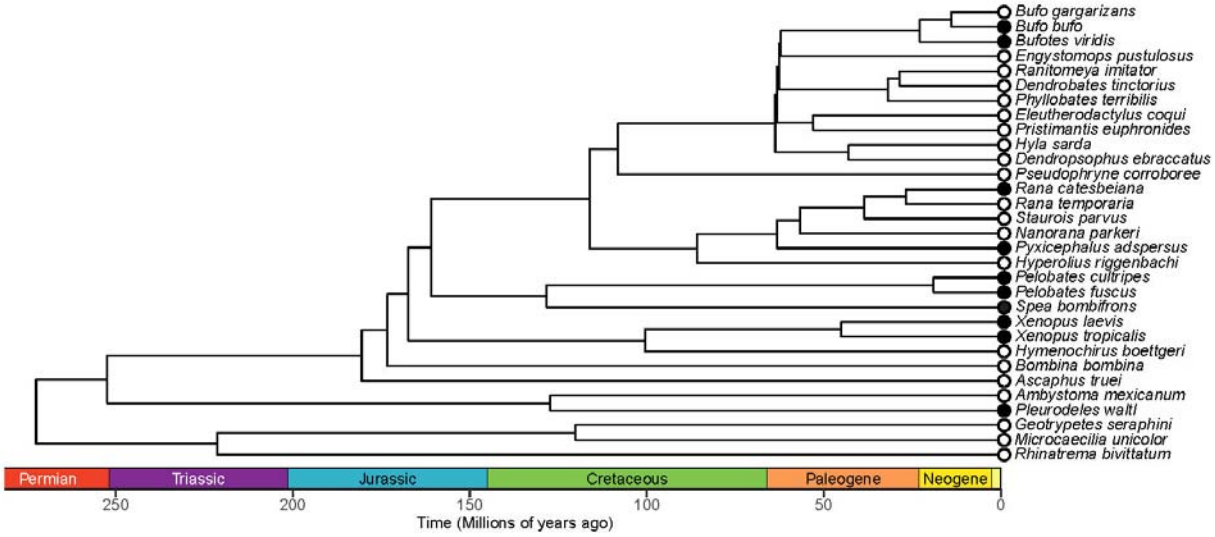

Figure 2

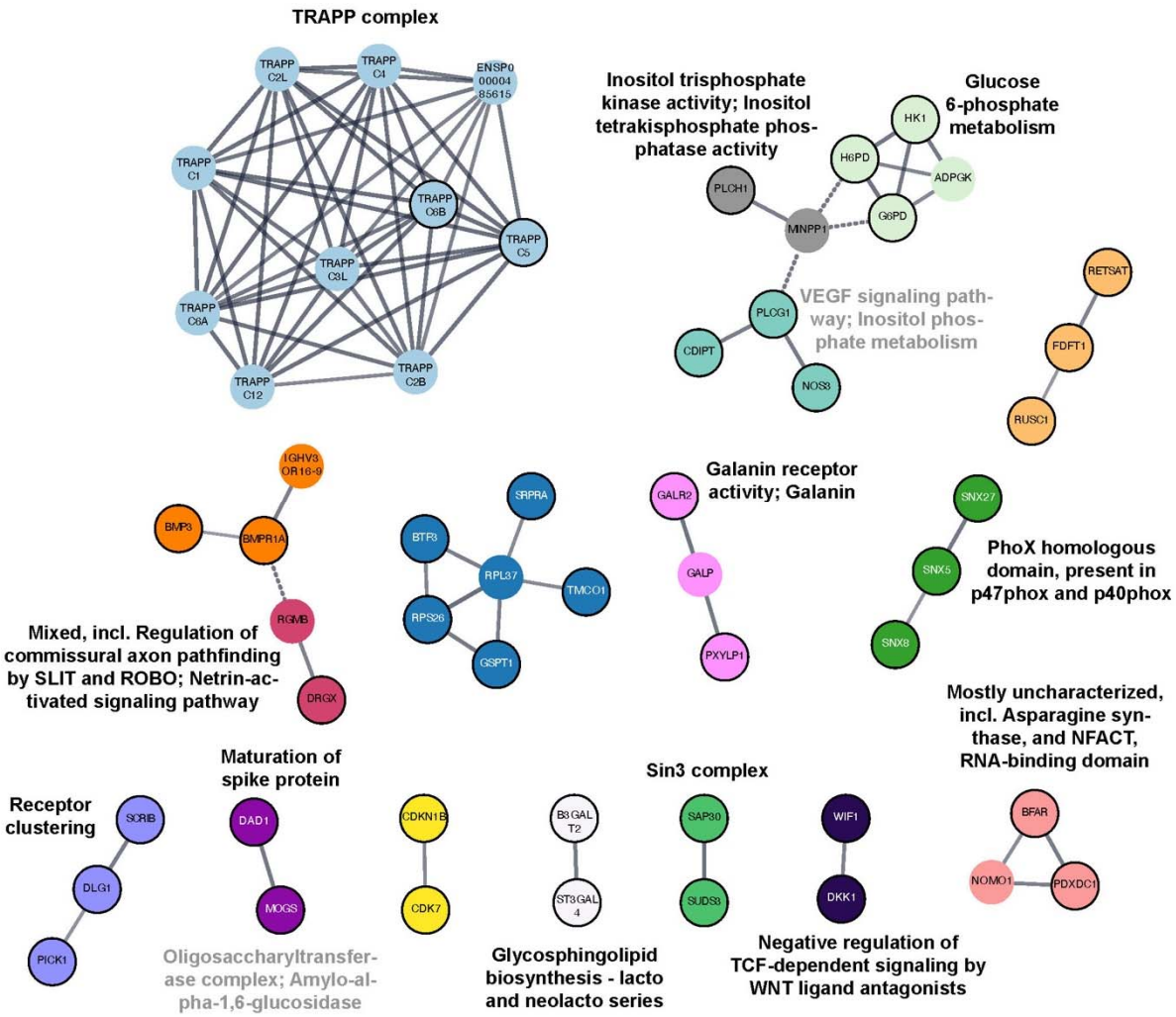
TRAPP complex
TRAPP C2L
TRAPP C4
ENSP0 00004 85615
TRAPP C1
TRAPP C6B
TRAPP C5
TRAPP C3L
TRAPP C6A
TRAPP C12
TRAPP C2B
Inositol trisphosphate kinase activity; Inositol tetrakisphosphate phosphatase activity
Glucose 6-phosphate metabolism
HK1
H6PD
ADPGK
PLCH1
MINPP1
G6PD
VEGF signaling pathway; Inositol phosphate metabolism
PLCG1
CDIPT
NOS3
RETSAT
FDFT1
RUSC1
IGHV3 OR16-9
BMP3
BMPR1A
RGMB
DRGX
Mixed, incl. Regulation of commissural axon pathfinding by SLIT and ROBO; Netrin-activated signaling pathway
SRPRA
BTF3
RPL37
TMCO1
RPS26
GSPT1
Galanin receptor activity; Galanin
GALR2
GALP
PXYLP1
SNX27
SNX5
SNX8
PhoX homologous domain, present in p47phox and p40phox
Mostly uncharacterized, incl. Asparagine synthase, and NFACT, RNA-binding domain
Receptor clustering
SCRIB
DLG1
PICK1
Maturation of spike protein
DAD1
MOGS
Oligosaccharyltransferase complex; Amylo-alpha-1,6-glucosidase
CDKN1B
CDK7
B3GALT2
ST3GAL4
Glycosphingolipid biosynthesis - lacto and neolacto series
Sin3 complex
SAP30
SUDS3
WIF1
DKK1
Negative regulation of TCF-dependent signaling by WNT ligand antagonists
BFAR
NOMO1
PDXDC1

Figure 3

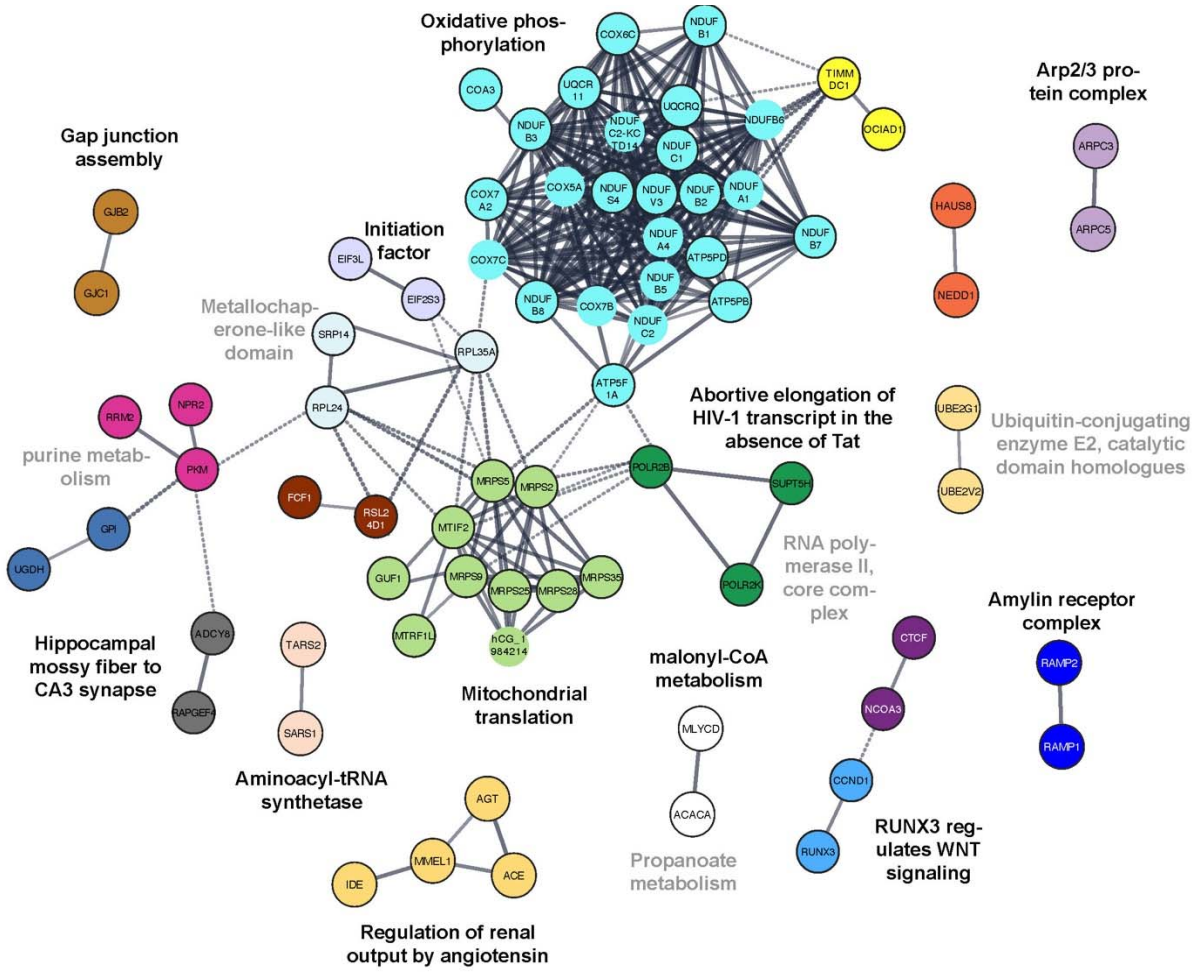
Oxidative phos-
phorylation
COX6C
NDUF
B1
TIMM
DC1
OCIAD1
COA3
UQCR
11
UQCRQ
NDUFB6
NDUF
B3
NDUF
C2-KC
TD14
NDUF
C1
COX7
A2
COX5A
NDUF
S4
NDUF
V3
NDUF
B2
NDUF
A1
NDUF
A4
ATP5PD
NDUF
B7
COX7C
NDUF
B5
NDUF
B8
COX7B
ATP5PB
NDUF
C2
ATP5F
1A
Arp2/3 pro-
tein complex
ARPC3
ARPC5
HAUS8
NEDD1
Gap junction
assembly
GJB2
GJC1
Initiation
factor
EIF3L
EIF2S3
Metallochap-
erone-like
domain
SRP14
RPL35A
RPL24
RRM2
NPR2
PKM
purine metab-
olism
GPI
UGDH
FCF1
RSL2
4D1
MTIF2
MRPS5
MRPS2
GUF1
MRPS9
MRPS25
MRPS28
MRPS35
MTRF1L
hCG_1
984214
Mitochondrial
translation
Abortive elongation of
HIV-1 transcript in the
absence of Tat
POLR2B
SUPT5H
POLR2K
RNA poly-
merase II,
core com-
plex
UBE2G1
UBE2V2
Ubiquitin-conjugating
enzyme E2, catalytic
domain homologues
Hippocampal
mossy fiber to
CA3 synapse
ADCY8
RAPGEF4
TARS2
SARS1
Aminoacyl-tRNA
synthetase
malonyl-CoA
metabolism
MLYCD
ACACA
Propanoate
metabolism
CTCF
NCOA3
CCND1
RUNX3
RUNX3 reg-
ulates WNT
signaling
Amylin receptor
complex
RAMP2
RAMP1
AGT
MMEL1
ACE
IDE
Regulation of renal
output by angiotensin

Figure 4

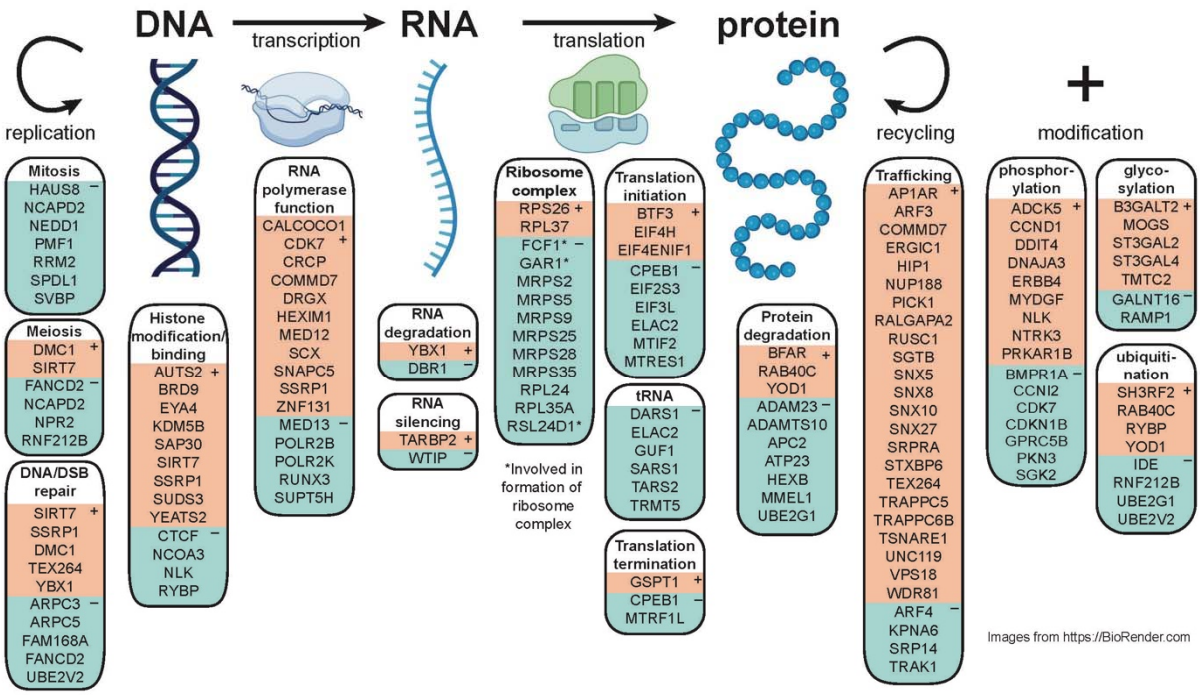
DNA
transcription
RNA
translation
protein
replication
recycling
modification
Mitosis
HAUS8 −
NCAPD2
NEDD1
PMF1
RRM2
SPDL1
SVBP
Meiosis
DMC1 +
SIRT7
FANCD2 −
NCAPD2
NPR2
RNF212B
DNA/DSB repair
SIRT7 +
SSRP1
DMC1
TEX264
YBX1
ARPC3 −
ARPC5
FAM168A
FANCD2
UBE2V2
Histone modification/ binding
AUTS2 +
BRD9
EYA4
KDM5B
SAP30
SIRT7
SSRP1
SUDS3
YEATS2
CTCF −
NCOA3
NLK
RYBP
RNA polymerase function
CALCOCO1
CDK7 +
CRCP
COMMD7
DRGX
HEXIM1
MED12
SCX
SNAPC5
SSRP1
ZNF131
MED13 −
POLR2B
POLR2K
RUNX3
SUPT5H
RNA degradation
YBX1 +
DBR1 −
RNA silencing
TARBP2 +
WTIP −
Ribosome complex
RPS26 +
RPL37
FCF1* −
GAR1*
MRPS2
MRPS5
MRPS9
MRPS25
MRPS28
MRPS35
RPL24
RPL35A
RSL24D1*
*Involved in formation of ribosome complex
Translation initiation
BTF3 +
EIF4H
EIF4ENIF1
CPEB1 −
EIF2S3
EIF3L
ELAC2
MTIF2
MTRES1
tRNA
DARS1 −
ELAC2
GUF1
SARS1
TARS2
TRMT5
Translation termination
GSPT1 +
CPEB1 −
MTRF1L
Protein degradation
BFAR +
RAB40C
YOD1
ADAM23 −
ADAMTS10
APC2
ATP23
HEXB
MMEL1
UBE2G1
Trafficking
AP1AR +
ARF3
COMMD7
ERGIC1
HIP1
NUP188
PICK1
RALGAPA2
RUSC1
SGTB
SNX5
SNX8
SNX10
SNX27
SRPRA
STXBP6
TEX264
TRAPPC5
TRAPPC6B
TSNARE1
UNC119
VPS18
WDR81
ARF4 −
KPNA6
SRP14
TRAK1
phosphor-ylation
ADCK5 +
CCND1
DDIT4
DNAJA3
ERBB4
MYDGF
NLK
NTRK3
PRKAR1B
BMPR1A −
CCNI2
CDK7
CDKN1B
GPRC5B
PKN3
SGK2
glyco-sylation
B3GALT2 +
MOGS
ST3GAL2
ST3GAL4
TMTC2
GALNT16 −
RAMP1
ubiquiti-nation
SH3RF2 +
RAB40C
RYBP
YOD1
IDE −
RNF212B
UBE2G1
UBE2V2
Images from https://BioRender.com